Designing For The Individual User: A Test Study for a 1:1 User-Centric Solution to the Problem of sEMG in the Forearm

by

Stuart Braiman

A Thesis Presented in Partial Fulfillment
of the Requirements for the Degree
Master of Science in Design

Approved April 2012 by the
Graduate Supervisory Committee:

Jacques Giard, Chair
Donald Herring
John A. Black Jr.

ARIZONA STATE UNIVERSITY

April 2012

ABSTRACT

All too often, industrial designers face seemingly intractable obstacles as they endeavor to, as Simon (1996, p. 111) describes, devise "courses of action aimed at changing existing situations into preferred ones." These problems, described by Rittel and Webber (1973) as "wicked," are insurmountable due to the contradictory and changing nature of their requirements. I argue that that industrial design (ID) is largely subject to Rittel's quandary because of its penchant for producing single solutions for large populations; such design solutions are bound, in some senses, to fail due to the contradictory and changing nature of large and, thus, inherently diverse populations.

This one-size-fits-all approach is not a necessary attribute of ID, rather, it is a consequence of the time in which it came into being, specifically, the period of industrial mass production.

Fortunately, new, agile manufacturing techniques, inexpensive sensors, and machine learning provide an alternative course for ID to take, but it requires a new way of thinking and it requires a new set of methods, which I will elaborate in this thesis. According to Duguay, Landry, and Pasin (1997), we are entering an age where it will be feasible to produce individualized, one-off products from large-scale industrial manufacturing facilities in a way that is not only cost effective, but in many ways as cost effective as the existing techniques of mass production. By availing ourselves of these opportunities, we can tame the problem, not by defeating Rittel's logic, rather by reducing the extent to which his theories are appropriate to the domain of ID.

This thesis also describes a test study: an experiment whose design was guided by the proposed design methodologies. The goal of the experiment was to determine the feasibility of a noninvasive system for measuring the health of the forearm muscles. Such a tool would provide the basis for assessing the true impact and possible pathogeny of the manual use of products or modifications to products. Previously, it was considered impossible to use surface electromyography (as opposed to needle or wire based electromyography) to assess muscular activity and muscular health due to the complexity of the arrangement of muscles in the forearm. Attempts to overcome this problem have failed because they have tried to create a single solution for all people. My hypothesis is that, by designing for each individual, a solution may be found. Specifically, I show that, for any given individual, there is a high correlation between the EMG signal and the movements of the fingers that, ostensibly, those muscles control. In other words, by knowing, with great accuracy, the position and the motion of the hand then it would become possible to disambiguate the mixed signals coming from the complex web of muscles in the forearm and enable the assessment of the forearm's health by non-invasive means.

DEDICATION

This thesis is dedicated to my wife, whose tireless effort and endless faith in me gave me the strength and courage to finish this project.

ACKNOWLEDGMENTS

I would like to acknowledge the following people without whose efforts I could not have completed this study: Jacques, John, Don, Panch, Michael, Gaurav, Vineeth, Dirk, and all of the members of the CUbiC lab.

TABLE OF CONTENTS

Page

CHAPTER Page

APPENDIX Page

LIST OF TABLES

LIST OF FIGURES

Figure Page

Figure Page

CHAPTER 1

INTRODUCTION

All too often, industrial designers face seemingly intractable obstacles as they endeavor to, as Simon (1996, p. 111) describes, devise "courses of action aimed at changing existing situations into preferred ones." These problems, described by Rittel and Webber (1973) as "wicked," are insurmountable due to the contradictory and changing nature of their requirements. I argue that industrial design is largely subject to Rittel's quandary because of its penchant for producing single solutions for large populations. Such design solutions are bound, in some senses, to fail, due to the contradictory and changing nature of large and, thus, inherently diverse populations.

This one-size-fits-all approach is not a necessary attribute of industrial design. Rather, it is a consequence of the time in which it came into being—specifically the period of industrial mass production. Industrialized mass production has been very successful in generating products for the marketplace at prices well below what had been possible before. It did so by leveraging economies of scale through the production of very large numbers of identical products. This strategy has become entrenched within the field of industrial design because of the price savings that it is able to generate.

Some products may, forever, remain ideal candidates for industrial mass production. Obvious examples are items in which there is little or no human-machine interaction. There may even be a substantial number of products with

which people interact intimately and intrinsically that are still viable candidates for industrial mass production, due to the shared or communal nature of their usage, or historical reasons for preferring a particular form. However, for the preponderance of products, the idea that single solutions should apply to all people has resulted in problems ranging from difficulty of use to, as is the case with the QWERTY keyboard, an epidemic of musculoskeletal disorders.

Amid the worst consequences of the mass-manufacturing model, no product is as glaringly problematic as the Sholes design, or QWERTY keyboard. This product has existed, in largely unchanged fashion, for well over a century despite tectonic shifts in the technology underlying the keyboard itself. It has been known since the very earliest days of typing on the Sholes design keyboard that severe musculoskeletal injuries can result from extended and frequent use of this product. In the early 1930s Dvorak, working with a team of industrial engineers, tested 250 keyboard variations and concluded that the Sholes design keyboard was "one of the worst possible arrangement[s] for touch typing" (Noyes, 1983, p. 263). But the keyboard's problems are not simply a matter of key position. Norman and Fisher (1982) found surprisingly little difference between keyboard layouts, concluding that improvements to the keyboard can only be made through a "radical redesign of the present physical key configuration" (Norman & Fisher, 1982, p. 509).

However, when one examines attempts to correct the design of this keyboard, it is clear that there are no universally agreed-upon metrics for quantifying the impact or efficacy of improvements. Additionally, given the vast

diversity of the human population, it is unlikely that any single design solution would be able to ameliorate the ergonomic shortcomings of the keyboard for every individual.

Fortunately, emerging technologies now provide an alternative course for ID to take, but it requires a new way of thinking and it requires a new set of methods, which I will elaborate later in this thesis. Agile manufacturing, one-off manufacturing, or mass customization; these are just a few of the many names for the large-scale manufacturing of unique products that can provide remedy for a seemingly intractable problem. According to Duguay et al. (1997), we are entering an age where it will be feasible to produce individualized, one-off products from large-scale industrial manufacturing facilities in a way that is not only cost effective, but in many ways as cost effective as the existing techniques of mass production.

In this thesis, I will lay the foundations for how one type of product, a keyboard-like input device, might be able to be designed manufacture in such a way that it meets the needs of an individual rather than the needs of the masses. Such a solution is possible as a result of two fundamental transformations in technology and manufacturing and a hypothesis about the human body that may allow us to overcome the current limitations in our ability to produce single products for each individual consumer.

The first relevant transformation underpinning the viability of my project is the dramatic reduction in the overall life cycle of products in our current, quickly changing product environment. Whereas in the past, the lifespan of a

product could have matched the lifespan of the machinery required to build it, today products become obsolete in such fundamental ways that the machines required to build them will be of use only for a fraction of the total lifespan of the manufacturing equipment.

The second relevant transformation deals with new technologies available for the large-scale determination of the attributes of differentiation that would characterize one-off products. There has been a dramatic reduction in both the cost and the size of sensors available to measure an individual's somatic attributes and responses. Simultaneously, there has been an explosive increase in computational power and techniques of pattern recognition and machine learning that enable an automated determination for the composition of products to ideally suit the needs of a single person.

Finally, a fundamental hypothesis that I explore in this thesis and throughout my research is that the body readily produces salient signals that can easily be measured by increasingly sophisticated sensors and that actionable interpretation of the body's signals can be performed by increasingly sophisticated machine learning techniques. This combination of factors results in a condition where one can foresee the type of work performed by earlier craftsmen—who made truly customized products—being accomplished with a programmatic workflow, cost-effectively for every individual, one at a time.

Now that the above conditions are coming to fruition, the field of industrial design could benefit from an expanded methodology for creating one-to-one (1:1) user-centric products. While the scope of this thesis does not permit

me to comprehensively elaborate such a methodology, I will propose some preliminary principles, referred to in this document as *continua*, which guided me in the development of a 1:1 user-centric solution. I elaborate upon each of these principles in detail in the Conceptual Framework section of the thesis.

This thesis is a test study for these proposed design methodologies. It is an attempt to attack a problem armed with the methodologies that I outline above. First and foremost, my proposed solution needed to leverage only information that is absolutely knowable about each individual rather than information gleaned from an archetypal understanding of all people since there is no evidence that the latter is of any value, especially given the near infinite variation found among human beings.

Originally, for this thesis, I intended to test the idea that the body could unselfconsciously reveal constitutional preferences and tendencies that could be used to generate a personal postural vocabulary, potentially to replace the keyboard. I hypothesized that if I were to monitor an individual's hand movements over a long enough period of time, a number of postures would emerge as comfortable, natural positions for the hand. I further hypothesized that if I were to create a custom input mechanism based exclusively on these postures that occurred most frequently, that use of such a device would produce a lower incidence of musculoskeletal pathologies than conventional keyboards, chording keyboards, or traditionally devised, one-size-fits-all postural vocabularies such as the American Manual Alphabet used in American Sign Language.

Unfortunately, such a project would be well outside of the scope of a Master's thesis largely because there is no generally accepted, noninvasive technique for assessing the ongoing impact of product use on the health of the muscles of the forearm. Such a technique is essential for adequately testing the real-world impact any novel solution. Currently, only assessment using needle or wire-based electromyography can accurately assess the health of the muscles in the forearm. But this technique is untenable for several reasons. First, the technique is so invasive that it would dramatically affect the possibility of attaining naturalistic, *in situ,* and unselfconscious behaviors in research subjects. Second, this technique currently remains out of reach of all but a few designers due to the expertise required to administer the needles correctly. Third, the technique involves the inherent difficultly of obtaining permission to conduct research, both from research subjects and from the Institutional Review Board for human research.

While my original research question revolved around how to use the principles of 1:1 user-centricity to improve or replace the Sholes keyboard, I needed to restrict the scope of my project. Therefore, in this thesis, rather then attempting to create an alternative keyboard I have endeavored to determine whether it would be possible to overcome the long-standing inadequacies of surface electromyography in the assessment of forearm muscle health through the use of 1:1 user-centric principles.

It is currently considered impossible to effectively use surface electromyography (sEMG)—as opposed to needle or wire based

electromyography—to assess muscular activity and muscular health due to the complexity of the arrangement of muscles in the forearm. That is, the overlapping layers and the sheer number of muscles in the forearm makes it impossible to determine with accuracy the source of an electrical signal captured on the surface of the skin. Specifically, it has been considered unlikely that sEMG could differentiate a strong signal from a muscle located deep within the forearm from a weaker signal originating from a muscle located closer to the surface of the skin.

And yet without a technique to assess the impact of an artifact's usage on the muscular health of the forearm, producing a truly 1:1 user centric manually operated product remains unlikely. I argue that if designers limit themselves to solutions that work for all people then the impasse might be impossible to overcome. But if we explore the possibility of solving this problem for each individual, one at a time, then a solution may be found.

I hypothesize that for any given individual there is a high correlation between the muscle activations and the movements of the fingers that, ostensibly, those muscles control. Such that, if you can measure the motion of a subject's hand with great precision and accurately synchronize that motion with the muscle firing of the forearm muscles it would become possible to disambiguate the mixed signals generated by the complex web of muscles in the forearm. This would provide a much needed, non-invasive tool to assess the impact of product usage on the upper extremity (the primary conduit for human machine interaction) using techniques easily accessible to industrial designers.

CHAPTER 2

LITERATURE REVIEW

Industrial design came into being in the late 1800s, during the beginnings of mass production. The net result of this timing is that industrial design became wholly centered on mass production (Ritchie & Black, 1999). Historically, this mass manufacturing took hold due to the dramatic reduction in cost that it secured by leveraging economies of scale, as well as the reduction in the cost of labor by the employment of unskilled workers (Mäkipää & Mattila, 2004; O'Grady, 1999; Pine & Davis, 1993; Sabel & Zeitlin, 1985). In large measure, industrial design has been a direct consequence of mass manufacturing.

Currently, however, a new type of industrial manufacturing is emerging through the leveraging of smart manufacturing techniques to produce products that are tailored to individual users, rather than a mass market. As early as the 1980s, futurists such as Alvin Toffler were predicting a "shift away from traditional mass production …accompanied by a parallel de-massification of marketing, merchandising, and of consumption" (Toffler, 1980, p. 254). Industrial design is increasingly able to achieve such a shift by re-envisioning the design and manufacturing process through means such as mass customization, a term coined by Davis (1987, p. 169), and defined as the situation whereby "the same large number of customers can be reached as in mass markets of the industrial economy, and simultaneously they can be treated individually as in the customized markets of pre-industrial economies." Furthermore, S. Brown, Lamming, Bessant, and Jones (2004, p. 120) paraphrase Fralix (2001) by noting

that “mass customization combines the best of the craft era, where products were individualized but at high cost, with the best of mass production, where products were affordable but highly standardized.” This new post-modern era of manufacturing and consumption means that end-users need no longer be satisfied with a one-size-fits-all product (Pine & Davis, 1993).

The research conducted for this thesis attempts to build upon the notion of mass customization and user-centric design and is aimed at demonstrating how recent techniques and methodologies can be employed to reap the greatest benefit from the promise of mass customization. As Da Silveira, Borenstein, and Fogliatto (2001, p. 6) note, technologies that enable mass customization include computer numeric control (CNC), flexible manufacturing systems (FMS), communication and network technologies such as computer-aided design (CAD), computer-aided manufacturing (CAM), computer integrated manufacturing (CIM), and electronic data interchange (EDI) (Hirsch, Thoben, & Hoheisel, 1998; Kanchanasevee, Biswas, Kawamura, & Tamura, 1997; King, 1998).

To motivate the transition to mass customization, it is instructive to review the unfortunate effects of the “one size fits all” model. I will focus principally on the typewriter/computer keyboard, including some of the human factors problems that have occurred due to industrial design’s past reliance on mass manufacturing principles in the design of this ubiquitous device. In particular, I will review the burgeoning literature on injuries resulting from repetitive stress, trauma, and fatigue during extended keyboard use, namely Cumulative Trauma Disorders (CTDs) and Repetitive Stress Injuries (RSI).

Today's computer keyboards are largely similar to the typewriter keyboards developed more than a century ago, in that the basic layout has not changed since that time (Amell & Kumar, 2000; Gerard, Jones, Smith, Thomas, & Wang, 1994). With his partners S.W. Soule and G. Glidden, Milwaukee newspaper editor Christopher Sholes patented the first typewriters to use a QWERTY keyboard in 1869 and the first models went into production in 1873 (Dirjish, 2008). Initially, Sholes had arranged the keys in alphabetical order from left to right, but at top speed, the typewriter keys would become entangled. Sholes rearranged the keys to the now familiar QWERTY arrangement to slow the typist, and reduce this problem (Dirjish, 2008). However, as Erdil and Dickerson (1997) note, the weak design of the QWERTY layout was discovered as early as the 1940s by Dvorak (1943), who listed the keyboard's disadvantages as follows: 1) overloading of the weaker left hand of right-handed typists, 2) overloading certain fingers and largely underutilizing others, 3) too little typing on the home row, and 4) excessive jumping back and forth by fingers from row to row.

Aside from these inefficiencies, the QWERTY keyboard has had disastrous effects on the health and productivity of office workers. As Fagarasanu and Kumar (2003, p. 120) note, although the keyboard is often non-adjustable, "it is used by nearly all computer users regardless of age, anthropometric characteristics, gender and performance, leading to increased musculoskeletal problems." More important, the ergonomic literature cites a strong correlation between typing and Cumulative Trauma Disorders (CTDs) such as Carpal Tunnel Syndrome (CTS) (Amell & Kumar, 2000; Burgess-Limerick, Shemmell, Scadden,

& Plooy, 1999; Fagarasanu & Kumar, 2003; Feuerstein, Armstrong, Hickey, & Lincoln, 1997; Fogleman & Brogmus, 1995; Hedge & Powers, 1995; Marklin & Simoneau, 2001; Serina, Tal, & Rempel, 1999), epicondylitis (Keir & Wells, 2002; Pascarelli & Kella, 1993), tenosynovitis (Szeto & Ng, 2000), and Work-Related Neck and Upper Limb Disorders (WRNULD) (Szeto & Ng, 2000).

Surprisingly, ergonomic research and attempts at redesign have been largely unsuccessful and, as Szeto and Ng (2000) note, some studies (Morelli, Johnson, Reddell, & Lau, 1995; Swanson, Galinsky, Cole, Pan, & Sauter, 1997) report no reductions in pain, or increases in efficiency, when using new versus old keyboards.

The figures for disease and loss of productivity due to use of the QWERTY keyboard are alarming. As reported by OSHA, repetitive strain injuries (RSI) cost more than $20 billion a year in worker's compensation, and currently comprise the most costly occupational health problem in the United States (Nainzadeh, Malantic-Lin, Alvarez, & Loeser, 1999). And, according to recent figures from the United States Survey of Occupational Injuries and Illnesses, Cumulative Trauma Disorders (CTDs) are increasing, and now account for nearly two-thirds of illnesses relating to the workplace (US Bureau of Labor Statistics, 1996). Melhorn (1994) as well as Muggleton and Allen (1999) note that the United States government predicted that CTDs will be recognized as the greatest risk to workers' productivity, in that it is estimated that roughly 50% of the workforce will have contracted them.

Predictions regarding the pathogenesis of CTDs has been complicated by difficulties in diagnosing and assessing them, partly due to an inadequate understanding of how and why CTDs occur. However, as Iridiastadi notes, "[L]ocalized muscle fatigue has received growing attention as a potential design variable and exposure metric in research towards prevention of musculoskeletal disorders in the workplace" (Iridiastadi & Nussbaum, 2006, p. 344). Other factors that have been found to correlate with the occurrence of CTDs include “repetitive motions, forceful exertions, and awkward postures” (Keyserling, Stetson, Silverstein, & Brouwer, 1993, p. 807).

Accurately assessing predictive factors such as fatigue, force, and awkwardness of postures remains a challenge. Self-report emerges as a particularly imprecise assessment, falling behind other methods (Spielholz, Silverstein, Morgan, Checkoway, & Kaufman, 2001, p. 588). However, attempts to find better methods have had limited success. S. Bao, Howard, Spielholz, and Silverstein (2006) conducted research on 733 human subjects and found that comparing self-report with alternative assessment methods (such as force matching with a force gauge or rating scales estimated by ergonomists) correlated poorly with these factors.

Defining “awkward postures” provides another methodological challenge since doing so often leads researchers into the same one-size-fits-all trap that is at the root of the CTD problem, due to a one-size-fits-all keyboard design. For example, although it is thought that hand postures outside of a “neutral position” lead to CTDs, as Brown notes, “the actual definition of ‘neutral wrist posture’ is

remarkably vague in the literature" (J. N. A. Brown, Albert, & Croll, 2007, p. 209). Furthermore, as demonstrated in Figure 1 where Bergamasco, Girola, and Colombini (1998) attempt to visually demonstrate non-neutral postures, such estimations are based upon a mass-user model that ignores physiological difference based on gender, height, body size, and age, among other factors.

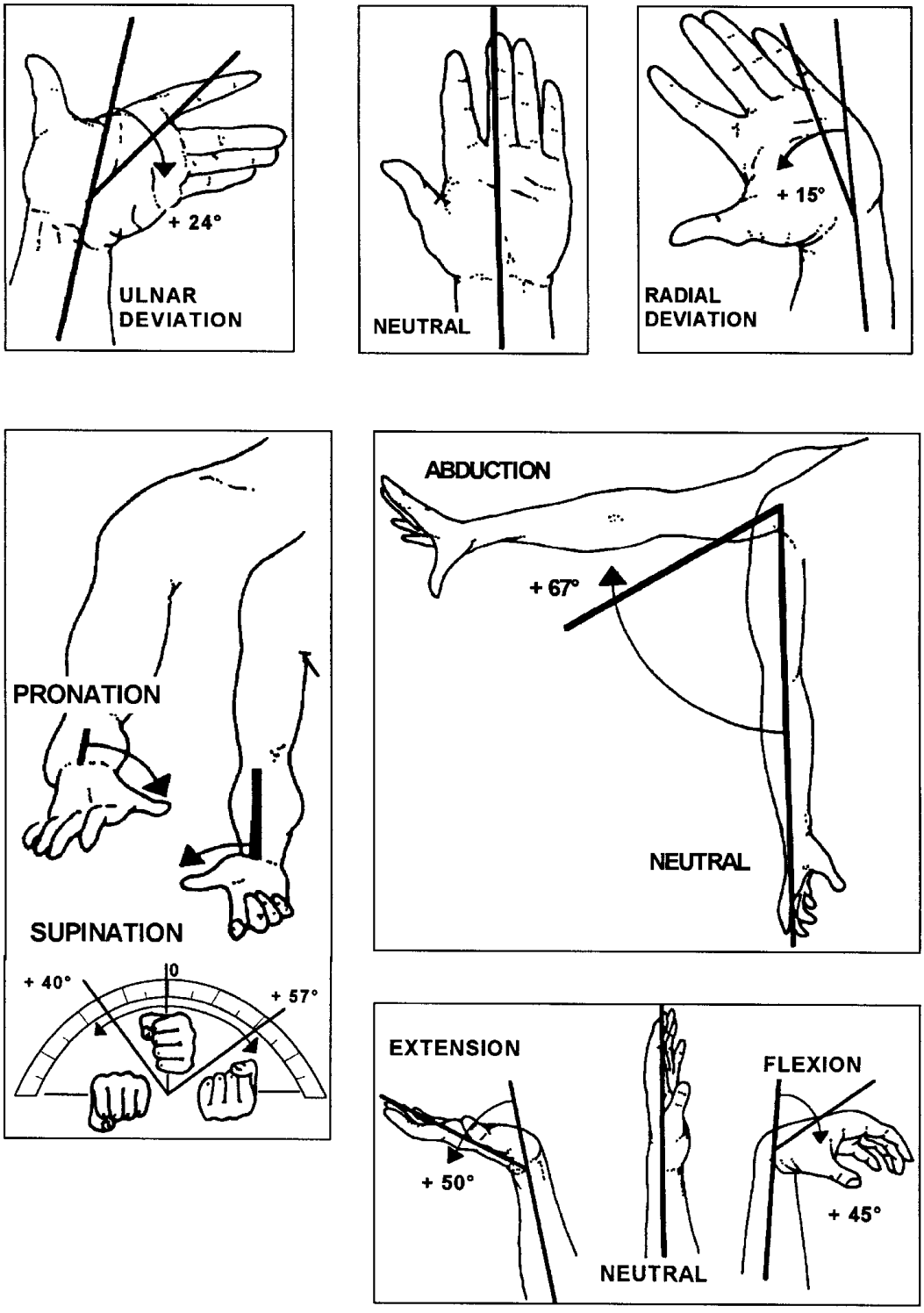

Figure 1. Positions of the arm deemed to be unacceptable (Bergamasco et al., 1998, p. 1366)

One method, however, seems to have more promise than others in assessing, diagnosing, and preventing CTDs. Electrodiagnosis using electromyography (EMG) has emerged as the "gold standard" (Fagarasanu & Kumar, 2003; Szabo, 1998). This is because EMG can be used to accurately and quantitatively measure the physiological factors inherent in repetitive hand motions, unlike other methods (Stephen Bao, Silverstein, & Cohen, 2001; Cook, Rosecrance, Zimmermann, Gerleman, & Ludewig, 1998). As Clancy, Morin, and Merletti (2002, p. 1) note, EMG signals have "been used to provide insight into musculoskeletal system function via estimation of muscle fiber conduction velocity, monitoring localized changes in the EMG during muscle fatigue."

However, when discussing EMG as a method, it is important to distinguish between invasive and surface EMG techniques. Whereas invasive EMG uses a wire or a needle, inserted through the skin and into the fibers of the muscle being examined, surface EMG (sEMG) is defined as "the study of muscle function through the electrical signals of the muscles, recorded with electrodes on the skin" (Basmajian & De Luca, 1985). It has been found to be effective for gaining information about 1) timing and intensity of muscle activation, 2) muscle fatigue, and 3) muscle force production (Basmajian & De Luca, 1985; Hermens, Hägg, & Freriks, 1997; Kamen & Caldwell, 1996; Ostlund, Yu, Roeleveld, & Karlsson, 2004).While it has been shown that sEMG is accurate for measuring muscle force and fatigue in large muscle groups, such as those found in the upper arm (Clancy et al., 2002), sEMG has not yet been successful at measuring force

and fatigue in complex, small muscle groupings, such as those found in the lower arm—an area essential to the understanding of CTDs among typists.

In areas like the forearm there is considerable "cross talk" between small muscles because the pick-up area of a sEMG sensor includes signals from muscles around the muscle being examined. This cross talk has proven to be very problematic. For example, as Ostlund et al. (2004, p. 825) note, "when more specific information about muscle activation is desired, surface EMG has traditionally been considered unsuitable, as today only limited information about single motor unit (MU) activity can be obtained. Therefore, in the field of neurophysiology, invasive (needle or wire) EMG is usually applied." And as Xu, Xiao, and Chi (2001, p. 30) write,

> [A]lthough surface EMG is non-invasive and is better accepted by patients – especially by children – the difficulty of identifying individual MUAPs [Motor Unit Action Potentials] from surface EMGs has significantly limited its application. Two main factors make the decomposition of surface EMGs difficult: (1) a low signal to noise ratio; and (2) significant superimposition of MUAPs.

This means that, when more than one muscle is present in the area being measured (most notably, the forearm), the only current EMG solution involves needles or wires, which are painful, invasive, and prevent the study of a research subject's natural forearm motions.

The experiment described in this thesis makes use of the CyberTouch glove for the collection of hand posture data. It is a light, comfortable, cloth glove with 18 thin foil strain gauges, developed by James Kramer at Stanford university

as part of a project to translate American Sign Language into spoken English (Sturman & Zeltzer, 1994). The CyberTouch glove allows for an accurate, stable reading of hand postures, "with resolutions within a single degree of flexion" (Sturman & Zeltzer, 1994, p. 34) including abduction and adduction, thumb crossover, palm arch, and wrist flexion (Dipietro, Sabatini, & Dario, 2008).

This thesis proposes to combine a CyberTouch glove with existing sEMG technology to investigate whether accurate, real-time hand posture data would support the development of mathematical techniques for reducing the cross talk in sEMG signals, allowing them to be used as a viable technology to accurately measure the conditions of forearm muscles.

CHAPTER 3

CONCEPTUAL FRAMEWORK

Industrial Mass Production

Around the mid 1800s, large machines were developed that were capable of quickly and cheaply producing identical parts. They required manpower, but the labor they needed was not same kind that had characterized production to that point. The term for these laborers was "unskilled" and, in conjunction with the industrialists that owned the plants, they quickly became solely responsible for the development of the artifacts people needed to go about their daily lives. It is true that more people were able to afford these new mass-produces items, but the craftsmanship that was present in earlier manufacturing was conspicuously absent.

Industrial Design's Legacy

As we enter the 21st century, many argue that mass production of goods is outdated (Pine & Davis, 1993). According to some assessments this "combination of single-purpose machines and unskilled labour to produce standard goods" (Sabel & Zeitlin, 1985, p. 133) has already been supplanted by dynamic/agile production techniques (Duguay et al., 1997).

Several new technologies now provide opportunities to overcome the decline in user customization that has been the hallmark of the mass production technologies of the last century and a half: (1) one-off manufacturing capabilities,

inexpensive, (2) small and low-power sensors, and (3) machine learning/pattern recognition. In my research, these technological advances are coupled with a working hypothesis that the human body can be monitored to detect the needs and intentions of its occupant. The resulting somatic information about each individual can be used to fine-tune artifacts to better meet the specific needs of each person, at a cost that approaches those of traditional mass manufacturing.

The Continua

Designing with this new paradigm involves two distinct stages. The first, which aims to produce a "rough draft" of a product, is not altogether dissimilar from traditional design research, which seeks to understand the problem to be solved, as well as the general needs, the physical features, and the cognitive characteristics of the target population. Decades of design research have yielded highly effective methods for this purpose.

However, the goal of this new paradigm of design does not end there. The second phase fully customizes this rough draft by ascertaining the specific needs and attributes of each individual through direct measurement. In the most advanced form, the rough draft of a 1:1 user-centric product is even able to customize itself, as it familiarizes itself with its intended user.

It is this second stage of the design process that is novel. New methods and principles are needed to guide the designer during this second stage toward the goal of providing a fully 1:1 user-centric product, one that fully meets the needs and satisfies the intended user.

Given the limited scope of a Master's thesis, I will not be able to fully detail a comprehensive set of parameters to guide designers aiming to take full advantage this new method of design. However, I will provide a list of factors, or *continua* that provided me with a roadmap, guiding both the research and the design process so as to fully leverage this new two-phase design paradigm. While not all design solutions can fall entirely on one side of each of these continua, I found that that by striving to maximize their location on the correct side of each scale I was most likely to be on the optimal path for 1:1 user-centric design. It should be emphasized that these continua influenced both the type of research questions I considered as well the physical instantiation of the artifact being designed.

Laboratory testing vs. *In Situ* testing

The ideal of *in situ* testing is to assess the effects of the actual behavior being examined, namely, the consequences of performing real work in real work conditions with the devices being tested. It is possible to estimate the efficacy of a design by devising laboratory procedures that accurately mimic some of the most important aspects of the work being performed. However, this is not the same as knowing what the actual effect on a specific person is when they perform work in the real world, unobserved and unselfconscious. It is only when we test the natural flow of work, unencumbered or distracted by invasive apparatus that researchers can measure the real way a device is used or exactly how a task is accomplished. As users, much of what we do in performing a task is not fully

obvious to us. Designers must be able to accurately describe and measure how users actually perform tasks.

Additionally, significant differences exist in the ways that various individuals perform a given task or operate a given piece of apparatus. Generalizations that form the basis for a laboratory experimental design might not be representative of all users, even if those generalizations are derived from careful and exhaustive observation of how a sample group performs a given activity.

True *in situ* observation allows the designer to measure how each individual is affected by the task at hand. This involves more than measuring the manner in which the individual performs the task in an isolated and controlled laboratory environment, but how that individual performs in the real world, unobserved and unselfconscious. The real world is the domain in which cumulative trauma disorders (CTDs) occur, and if the designer wishes to determine the likelihood of pathology, and use this information to inform the design of products, then the designer must conduct observations in this domain. In sum, we must measure real work, with real devices, over real periods of time, for real individuals, one at a time.

Example: In the past, when performing analysis of tasks done with the forearm and hand, invasive needle-based electromyography (EMG) has been seen as the only option. The alternative method of surface-based EMG has not been deemed to be adequate due to the difficulty of sorting out the blend of signals produced by the complex, layered, and interwoven set of muscles in the forearm.

Consequently, measurements of muscle activity in the forearm and hand during manipulative tasks needed to be done in a laboratory environment by a trained practitioner, under stringent limitations imposed by the local Institutional Review Board (IRB). Past research done by such practitioners are of limited value to the industrial designer because they are typically limited to measurements of stereotypical hand postures and the forces generated by stereotypical activities such as maximum voluntary contraction or static posture generation. Also, due to the fact that needles are inserted into the forearm, many precautions must be taken to ensure that no pain is inflicted on the subject, and that no damage is done to the subject, including muscle tearing or risk of infection.

Objective vs. Self-Report

As discussed in the literature review section, research has shown that self-report is highly problematic for identifying root causes of pathologies. With RSI/CTD in particular, clinical evidence shows that the early stages of fatigue, which are a precursor to RSI/CTD are rarely identifiable by people and, when identified, rarely described in a useful way. Thus, the traditional use of self-report is of limited value to designers who seek to develop products that avoid RSI/CTD.

For this reason, the filter of narrative self-report must be bypassed in favor of direct and objective observational methods so as to maximize the collection of accurate and actionable data. A person's subjective choices regarding how to speak about their sensations (either because of personality type or their disposition on a given day) must be removed from the equation. If multiple tests

are to be performed on a given person, or testing of multiple designs, then truly objective measurement is required to make comparisons in real-world, *in situ* work conditions. It is important that a test measure the actual task in as much as possible, exactly as the task would be performed once a person takes a product home (or to the office) and goes about their business unobserved.

Qualitative vs. Quantitative

Much of what designers do involves the qualitative improvement of people's lives. Since we deal with improving the lot of human beings, not everything can be quantified perfectly. However, when it comes to the onset of pathologies it is important to employ quantitative measures to ensure that a new product or the alteration of an existing product does not produce serious or even inconvenient health issues.

As stated in the objective vs. self-report dichotomy, it is important that information derived from product testing provide an objective basis of comparison. If a product is modified, then the positive or negative effects of that modification on that person need to be able to be quantified. The problem with qualitative measures is that the same person doing the same task on two different days is likely to give different qualitative descriptors.

Also, it is important to note that qualitative measurements tend to be less specific than their objective counterparts. A general feeling of tiredness or a lack of well being or a feeling of "resonance" is not as helpful in guiding the design

process as quantitative data that indicate mathematically articulated levels of fatigue.

In addition, given that this new design paradigm includes the possibility of a final phase of self-customization, which is accomplished programmatically, it is imperative that any factors that are important to the customization process be accessible to the intelligent, computer-controlled product.

Example: Qualitative assessments generally yield only warmer/colder types of metrics. They are often one-dimensional in nature, and improvements to one part of the body might be harmful to others. This has been particularly problematic with keyboard modifications. A study that identified excessive strike force required for hitting keys as a factor in musculoskeletal pathogenesis recommended reducing the energy required for depressing the keys. This modification resulted in the chronic use of other muscles to prevent accidental key activation. Whereas the earlier design allowed the user to rest their hands on the keyboard without inadvertently activating the keys, now the hands had to be continuously supported, almost in mid-air. The result was a more severe problem than the one the researchers attempted to ameliorate. By appealing to a more objective method of inquiry, discrete and high-dimensional data can be collected to identify when proposed modifications to ameliorate one problem might exacerbate another.

Individual vs. Population

Individuals differ from each other in significant ways. What might be good for one might be less than ideal (or even harmful) to another. This even applies to individuals as they progress through their lives. Whether due to the changing anthropometry of maturation or to the progressive degeneration that takes place after development is complete, a person is continuously changing over time. Tests that determine the likelihood of pathology must be able to assess effects on individuals and those effects must be recognized as specific to that person only at the moment of testing.

Generalized models are useful for quantifying variances across populations but they were developed to support the old mass-manufacturing paradigm of industrial design. There is no guarantee that age projection or identifying a person's uniqueness as an extrapolation of a population-based archetype yields accurate information about an individual. The new proposed paradigm of industrial design demands extensive testing on individuals *qua* individuals so as to do justice to their uniqueness and, thereby, give an accurate indication of the real effects of a product or task on each individual.

Real-time vs. Longitudinal

It is important to make determinations of possible pathogenesis as quickly as possible during the exploration phase of the design process. Traditionally, assessments of design changes require a longitudinal study. If real-time techniques can be developed, iterative development techniques can be used

throughout the process, and can guide design changes no matter how minor they are.

If tests for the efficacy of a design alteration take months, the number of possible design iterations that can be tested shrink to a small number. Not only is the number of design directions severely curtailed, the number of iterations that can be tested in any given direction is severely reduced in even the most generous of budgets and design schedules.

Overcoming problems collecting forearm data with sEMG

Unlike previous attempts at addressing ergonomic problems with the keyboard that use entire populations as the basis for design intervention, this thesis proposes an alternative solution that examines individuals in the course of doing real data entry work in real time. Surface EMG has been widely used to measure the effects of work on large muscles throughout the body. However, its application in assessment of the muscles of the lower arm and hands has been less successful.

A major problem with collecting sEMG data from lower arm musculature is "cross-talk" between the individual muscle signals. The hypothesis that guides the proposed approach is that there are enough correlations between the activity of the muscles in the forearm and hand movements to allow for successful separation of the sEMG signals from the various muscle groups in the forearm, allowing their independent activities to be tracked with the separate signals.

What follows is a detailed description of the conceptual underpinnings of the experiments conducted to determine whether there is sufficient correlation between an individual's hand motion and the corresponding sEMG signals to merit further research on this approach.

Collecting Accurate Data

It was essential in my experiment to ensure that: (1) the collection of hand posture data was accurate, (2) that the resolution was adequate, and (3) that the data collection was precisely synchronized with the collection of sEMG data from the forearm. In order to ensure this, appropriate software, and hardware was developed and integrated.

CyberTouch Glove

As mentioned previously, it was important for my experiment design to collect accurate hand posture data in real time. Currently, one of the most effective ways of capturing hand posture data is the CyberTouch glove from Immersion Corporation. This instrumented glove is fairly unobtrusive and lightweight (weighing only 3 ounces). It is constructed from a thin elastic fabric, with a mesh back for ventilation. The 18 sensor model (used in this experiment) has open fingertips facilitating typing, writing, grasping of objects, or other manual tasks. It is equipped with 18 proprietary resistive bend-sensing strips that are sewn into the fabric of the glove. Each of these strain-gauge sensors is a long thin strip of metal whose resistance varies in proportion to the degree to which it is bent. A driver detects changes in its resistance to an electric current passed

through the strip and translates the measure of resistance into the angle of bending between the two ends (Kramer, Lindener, & George, 1991).

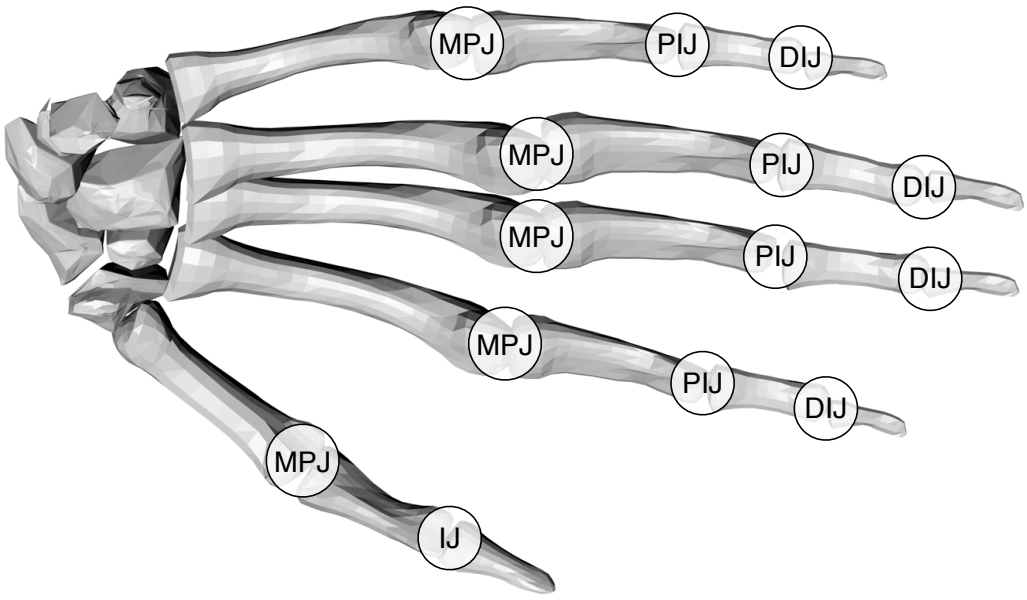

Figure 2. Diagram of hand bones labeled to show the joint-angle sensor locations of the CyberTouch

The 18 sensors are distributed across the glove as shown in Figure 2. The four (non-thumb) fingers have two sensors that measure the bend of the *metacarpophalangeal* (MCP) and *proximal interphalangeal* (PIP) joints. These are the two joints of the finger closest to the palm. Additionally, there are three *abduction* sensors between adjacent fingers that measure how widely these two fingers are laterally. The thumb has two sensors: one to measure the bend of the MCP and *interphalangeal* (IP) joints, and another to measure the rotation of the thumb across the palm, toward the pinkie finger. Two sensors at the wrist measure the pitch and the yaw of the palm, with respect to the wrist (referred to as wrist

flexion and wrist abduction, respectively). A sensor is also used to measure how much the pinkie rotates across the palm in the direction of the thumb (this measurement corresponds to the arch of the palm near the pinkie finger when the hand is cupped). Table 1 shows the CyberTouch sensors descriptions with their corresponding numerical labels.

Sensor #	Sensor Name (Description)
1	thumb rotation/TMJ (angle of thumb rotating across palm)
2	thumb MPJ (joint where the thumb meets the palm)
3	thumb IJ (outer thumb joint)
4	thumb abduction (angle between thumb and index finger)
5	index MPJ (joint where the index finger meets the palm)
6	index PIJ (joint second from finger tip of the index finger)
7	middle MPJ (joint where the middle finger meets the palm)
8	middle PIJ (joint second from finger tip of the middle finger)
9	middle-index abduction (angle between middle and index fingers)
10	ring MPJ (joint where the ring finger meets the palm)
11	ring PIJ (joint second from finger tip of the ring finger)
12	ring-middle abduction (angle between ring and middle fingers)
13	pinkie MPJ (joint where the pinkie finger meets the palm)
14	pinkie PIJ (joint second from finger tip of the pinkie finger)
15	pinkie-ring abduction (angle between pinkie and ring finger)
16	palm arch (causes pinkie to rotate across palm)
17	wrist pitch (flexion/extension of wrist)
18	wrist yaw (abduction/adduction of wrist)

Table 1. CyberTouch sensor identification table

The glove is connected with a cable to an interface box that translates the resistance value of each sensor into a value between 0 and 255. According to the manufacturer, the typical hand will produce values between 40 and 220, thereby allowing “headroom” for hands that flex or extend beyond what would be expected from a “typical hand.”

Overcoming Problems with the CyberTouch

The CyberTouch interface box only contains a single Analog-to-Digital Converter (ADC) that serially samples the current flowing through each of the 18 joint angle sensors in the glove. The ADC converts that current (which is inversely proportional to the resistance of that sensor) into a digital number between 0 and 255. This sampling is performed for one sensor at a time. As such, though the data files generated by the CyberTouch glove imply that all 18 data points were collected at the time indicated by the time-stamp, the glove does not take a single snapshot of the entire hand at a single point in time. What actually occurs is that when the ADC finishes sampling all 18 of the sensors, it assigns a single time-stamp and stores all of the results in a single record, along with that time-stamp; regardless of the actual time each sample was collected.

The consequences of this single timestamp are the possibility that (1) the joints that were sampled early in the serial sampling might have moved slightly by the time the time-stamp is created, and (2) if the hand was moving quickly enough it would be possible that the hand was never in the exact posture represented by the 18 stored values at any given time. In fact, it is possible (though unlikely) that the 18 stored values might even represent a hand posture that the given individual is physiologically incapable of generating.

Because I needed to be able to record rapid hand movements accurately, I needed to develop a method for recording the exact moment that the ADC sampled the resistance of each sensor. Investigations into the CyberTouch itself revealed that there was a pulse available on a secondary port of the CyberTouch

Interface Box, a *sync pulse* that identified the exact moment that each bend sensor was sampled. With this pulse I was able to develop software and hardware to determine the exact time that each sensor was measured.

Surface Electromyography (sEMG)

Finding the location of the muscles

To find the location of the muscles for each subject, I had them perform both "piano" and "scratch down" movements (described below) with each of their fingers separately, and also all together. As they performed these movements, I palpated their arm to find the bellies of all of the flexor muscles, to accurately apply the sEMG sensors to the skin within sensing range of all active muscles.

For the pinky and index fingers, there are two additional muscles that control extension: Extensor Digiti Minimi and Extensor Indicis, respectively. To localize the bellies of these two muscles for optimal placement of the sEMG sensors, I asked the subjects to perform the same two piano and scratch down motions with these two fingers.

Filtering

No filters were used to remove noise within the main frequency of the signal. It is true that some 60 Hz hum was present in the signal and, throughout the literature, a notch filter is recommended for removal of this noise component. However, there was a significant amount of electromyographic signal present in that frequency range, and arbitrary removal of all 60 Hz data would have removed

key data regarding the activity and condition of the muscle. Since the 60 Hz electrical noise is relatively constant and thoroughly independent of the motions of the subject's hand, the lack of correlation was judged to be sufficient to distinguish the signal from the noise.

A Butterworth filter was used to remove frequency components that are not normally present in the sEMG signal.

Synchronization of Clocks

The Master Clock

The collection of data required the use of two systems, each of which was mediated by its own internal clock. In order to allow synchronization of the data streams collected by the EMG and the glove, some method was needed to align the two sampling clocks of the EMG system with the sampling clock of the CyberTouch system

I chose to designate the DAQ1 clock signal of the EMG system as the "master clock." The DAQ2 clock signal of the EMG system was then synchronized to this master clock as described below.

In addition to the hand posture data provided through its serial port at the end of each 18-sensor scan, the CyberTouch interface box provided a secondary port with a narrow sync pulse that indicated the *exact moment* that each of the 18 strain-gauge sensors was sampled. Although very accurate, this narrow sync pulse it could not be reliably sampled by the ADC in the EMG system, and, therefore,

could not be incorporated into the EMG data set. Below is a diagram of the analog signal referred to as the synch pulse.

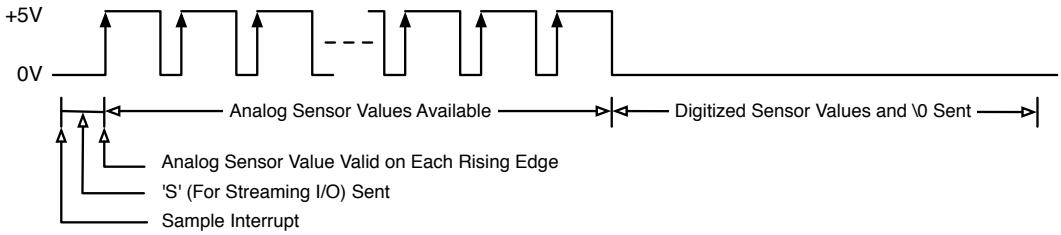

Figure 3. Sync Pulse Signal

As Figure 3 shows, there are 18 sync pulses that mark the moment of sampling for each glove sensor. The sampling rate of the ADCs in the EMG system was too low to reliably detect the narrow drop between these sync pulses, causing 40% of these drops to be missed. One possible solution would have been to replace the EMG system with one whose ADC sampling rate was much higher. However, the cost of such a system was well out of the reach of the lab.

To allow the EMG's ADC to reliably detect the sync pulses, I built the timing circuit shown in Figure 4 (from hereon referred to as the *pulse stretcher*) to extend the duration of the signal long enough for it to be consistently and reliably detected at the 2,000 samples per second rate of the EMG's DAC.

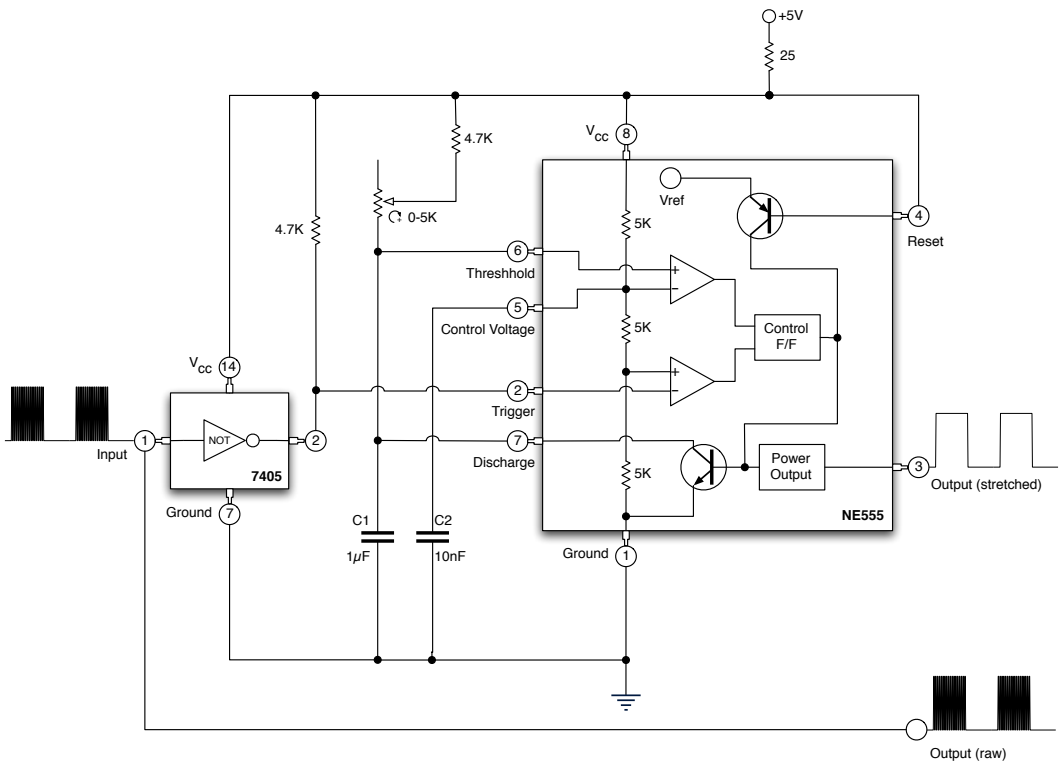

Figure 4: Pulse Stretcher

This pulse stretcher captured the sync pulse signal from the CyberTouch control box and produced the following two outputs:

- The original, unmodified pulse signal (from hereon referred to as the *sample pulse*) identifies every time a joint-angle measurement is made from one of the strain-gauge sensors. This signal is of a very high frequency and requires a high sampling rate to accurately digitize.
- A stretched pulse (from hereon referred to as the *frame pulse*) identifies the time interval during which all 18 glove sensors were sampled. This frame pulse can be reliably sampled at 2,000 samples per second, which was determined to be the optimal sampling frequency for surface EMG signals in this experiment.

The frame pulse was used to identify the time at which the first of the 18 samples was taken from the glove. The frame pulse was sampled by the ADC in the sEMG system, and stored along with all the EMG signals so that the timing of the first of the 18 joint angle measurements was known with respect to the sEMG clock. The timing of the remaining 17 pulses was then calculated as an offset from the first sample. In this way, the sEMG signals were collected at their optimal sampling frequency, and the hand position data from the CyberTouch was collected at its highest possible resolution, while ensuring that a single clock indicated the time that these events took place. The details of these calculations are described later, in the Results section.

Synthetic, "Arbitrary-Time" Hand Position

Even though a single clock indicated the exact timing of both the sEMG data and the hand posture data samples, the exact times at which these samples were taken were not identical. In order to have a "snapshot" showing the exact posture of the hand at the moment that each sEMG sample was taken software was developed to "interpolate" the sampled values for the joint-angle measurements corresponding to the exact time that each sEMG sample was collected.

While there are several mathematical options available for interpolation, linear interpolation produces discontinuities, as shown in Figure 5. If such an interpolation were plotted over time it would produce very "jerky hand movements. An interpolating method that produces smoother transitions between

data points is preferable. For generating smooth hand posture representations I chose to use *cubic interpolation*.

Cubic interpolation results in transitions much more typical of the type of motion produced by the human hand. This is clearly visible when comparing cubic interpolation as shown in Figure 6 to linear interpolation as shown in Figure 5.

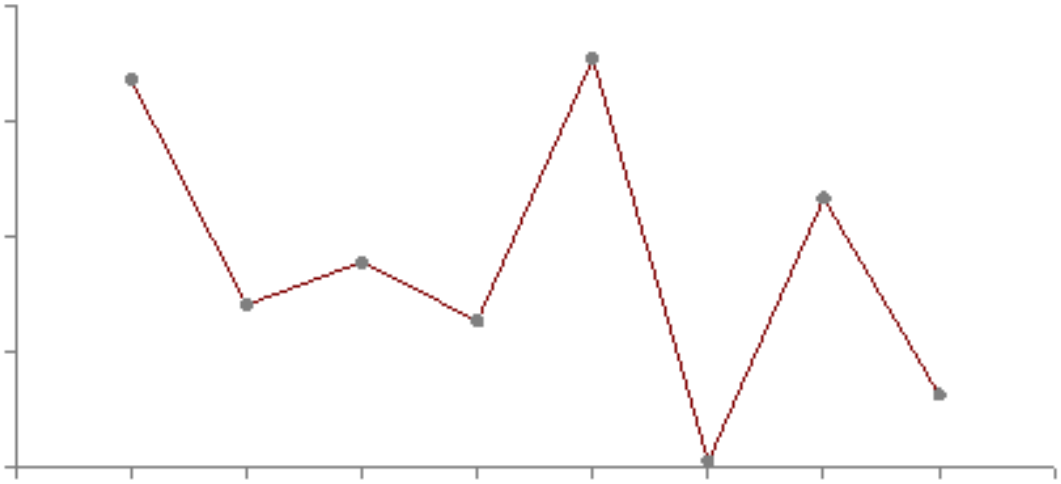

Figure 5: Linear interpolation (Bourke, 1999)

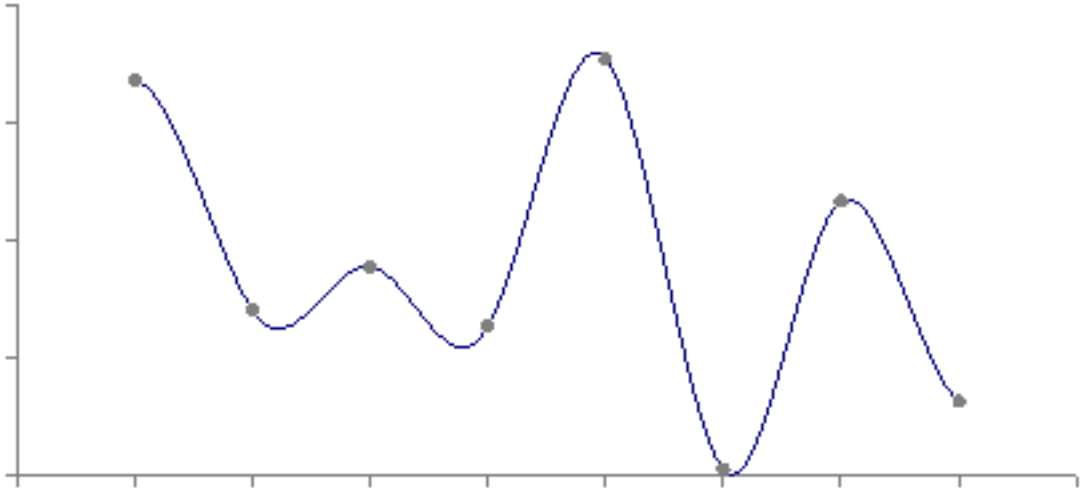

Figure 6: Cubic interpolation (Bourke, 1999)

Motion Primitives

In order to facilitate the measurement of correlations between the sEMG signal and the hand position data from the CyberTouch, it was important begin the experimental procedure with a small set of movements—each devised to evoke the activation of a single muscle or, at the very least, as few forearm muscles as possible. These "motion primitives" were comprised exclusively of movements of the four non-thumb fingers. To minimize interference from other muscle activations, the thumb, the wrist, and forearm were immobilized with a brace in such a way that was comfortable and relaxing enough that no muscular activity was required in order to maintain their position.

The motion primitives that I selected were based on anatomical observation of the ligaments' attachment to the digits. Specifically, motions were created that would activate the muscles associated with each ligament. For each ligament, flexors and extensors were isolated from each other, and both slow and quick motions were used during the data collection process. The faster the muscle movement, the more exertion is required and, therefore, the higher the amplitude of the EMG signal produced by such a movement. Conversely, slow movement is easier to produce without needing to simultaneously activate other muscles to maintain the positions of the remaining digits.

A total of 8 motion primitives were used to collect EMG data for each of the 4 non-thumb fingers, for a total of 32 motion primitives. The motion primitives were as follows:

1. index finger
    1.1. piano down slow
    1.2. piano up slow
    1.3. piano down fast
    1.4. piano up fast
    1.5. scratch down slow
    1.6. scratch up slow
    1.7. scratch down fast
    1.8. scratch up fast
2. middle finger
    2.1. piano down slow
    2.2. piano up slow
    2.3. piano down fast
    2.4. piano up fast
    2.5. scratch down slow
    2.6. scratch up slow
    2.7. scratch down fast
    2.8. scratch up fast
3. ring finger
    3.1. piano down slow
    3.2. piano up slow
    3.3. piano down fast
    3.4. piano up fast
    3.5. scratch down slow
    3.6. scratch up slow
    3.7. scratch down fast
    3.8. scratch up fast
4. pinkie finger
    4.1. piano down slow
    4.2. piano up slow
    4.3. piano down fast
    4.4. piano up fast
    4.5. scratch down slow
    4.6. scratch up slow
    4.7. scratch down fast
    4.8. scratch up fast

Cataloging the Motion Primitives

Pilot studies showed that it was awkward and impractical to mark the beginning and the end of the performance of each of the motion primitives during the experiment. Instead, a video camera capable of collecting timecode as well as a capture rate of 60 frames per second was used to document the experimental procedure. The video data were analyzed frame-by-frame in Apple Final Cut Pro and the timecode for the exact frame was noted in a worksheet for the beginning and end of each motion primitive. Because the directions of the up and down motion primitives were opposite in motion only 16 of the 32 primitives required visual labeling (e.g., *piano slow*, *piano fast*, *scratch slow*, *scratch fast*).

Synchronizing the Motion Primitives to the Master Clock

Clock synchronization was accomplished by having the subject perform an action that would be easy to identify in both the CyberTouch data stream as well as the video stream. The subject's hand was placed on the padded arm of an ergonomic office chair, which was adjusted for the most relaxing position, per the subject's verbal report. Once the subject's hand came to a complete stop and was free of any observable movement (or movement indicated by the CyberTouch), the subject was asked to clench their fist as quickly and as tightly as possible. As is shown in Figure 12, this movement is clearly identifiable in the CyberTouch data stream. The exact time that this motion began was extracted from the CyberTouch data, and was matched with the first video frame in which motion took place. Since the CyberTouch data had already been synchronized with the master clock, the new video data was, by extension, synchronized with the master clock as well.

Data Integrity from Custom Software

In addition to overcoming the accuracy limitations of the supplied software mentioned earlier, the custom software also allowed for the CyberTouch data to be input directly into MATLAB, allowing for quality assurance to be performed during the experiment itself, and allowing for future options such as real-time analysis of the captured data.

Dropped or Malformed Data

Early experiments suffered from buffer overflow issues with the serial port. Contingencies needed to be made for dropped or malformed data. Although later revisions to the software resulted in error-free data capture, the possibility of malformed data could obviate long and potentially unrepeatable experiments. MATLAB code was written to find abnormalities in the data. The code would try to fix the problem, or it would delete questionable segments of data and then ameliorate the problem by restructuring the subsequent data so that it was usable from that point forward.

Abrupt Termination

It was also important to take precautions against abrupt termination in the data collection. In the case of power loss or a system malfunction, particularly relevant during lengthy data collection sessions, data was written directly to disk and in such a way that the data files maintained their efficacy even if the data collection process terminated prematurely.

Calculating Acceleration

It is my hypothesis that stronger correlations with muscle activation can be found with the *acceleration* of the joints of the hand rather than the *position* of the joints. Once a hand is in a particular position, the muscle activations that were required to get it there are no longer being used. Therefore, the same hand position could have dramatically different accompanying muscle activations

depending on whether the hand is (1) stationary, (2) in the beginning of a motion, (3) coming to a stop, or (4) at any of the numerous stages of its movement. While it might be true that, in particularly awkward positions, some continuous muscle activations might be required just to keep fingers in a particular position, the type of muscle activation required to keep a posture would be different than that required to generate movement of the hand into that position. Thus, I hypothesized that it is not simply the motion of the hand that is most related to the muscle activity, but rather it is the acceleration (i.e., changes in the motion) of the hand that would yield the strongest correlations with muscle activity.

For this reason, the moment-by-moment positions of the hand were converted into moment-by-moment velocity data, which, in turn, were converted into moment-by-moment acceleration data. Deceleration is simply negative acceleration provided by activating antagonist muscles so that, as a finger comes to the end of its flexion, activations of extensor muscles contribute to the acceleration during the final moments of that motion.

CHAPTER 4

METHODOLOGY

Apparatus

The equipment used to test the hypotheses underpinning this study was built for small fraction of what a turnkey solution would have cost (~ 3%). It required the design and construction of custom circuits to maximize the degree of synchronization for the disparate data streams. Custom software was also written to overcome inaccuracies in the data reported by the CyberTouch as well as to maximize the resolution of the hand posture data. A detailed description of the apparatus is included in Appendix A.

Participants

A total of five subjects participated in this study. Three of the participants were male and two were female. The ages of the participants ranged from 21 to 55 years of age and represented various national/ethnic origins. None of the participants were compensated for their participation.

Calibration

Baseline Calibration was performed by generating a continuous zero volt signal from within the EMG unit while signals were sampled with the NI DAQ and routed to a LabVIEW application that monitored voltage and calculated the average of the incoming samples. 20,000 samples were taken at a rate of 2kHz

(for a total of 10 seconds). The averages were calculated for each channel, and adjustments were made to the amplifier's baseline setting. Tests continued until the averages were within 1% of 0V.

Gain Calibration was performed by generating three alternating positive and negative 100μV spikes. They were amplified by a factor of 10,000. 20,000 samples were taken at a rate of 2kHz (for a total of 10 seconds). Minimum and Maximum values were calculated for each channel and adjustments were made to the amplifier's gain setting. Tests continued until minimum and maximum values were within 1% of 1V.

After calibration with the test signals, signals from a single pair of sensors were routed to the seven amplifiers to test the signal stability of each of the sensors with respect to each other.

Explanation and briefing

Once the experiment appointment was scheduled with a subject, each participant was given a handout giving a brief background on the study. It was explained that the purpose of the experiment was to determine if accurate measurements of the lower arm's muscles could be achieved via surface electromyography (sEMG) when the addition of information about the hand's posture, velocity, and acceleration was included in the analysis.

In addition, information was given to subjects regarding the length of the experiment, as well as specific requests, such as wearing a loose, short-sleeved shirt, removing jewelry, and refraining from using lotion (e.g., sunscreen, creams,

or oils) on the arm or hand (areas where sEMG sensors will be attached) for a period of no less than 24 hours prior to the time of testing.

For a detailed transcript of the script used to coach participants, refer to Appendix 2.

Initial data intake

Before beginning the experiment, several demographic questions were asked of the subject. These included age, ethnic association/country of origin, sex, and handedness. The subject was also asked questions regarding their (1) level of physical activity, (2) self perception of upper extremity strength, and (3) experience of any type of repetitive stress injury (RSI) or cumulative trauma disorder (CTD).

Preparation of the subject

The optimal location for the placement of the EMG sensors on each individual was determined by palpating the general area of the muscle in question while the subject was asked to move their fingers similarly to the way they would be asked to move them during the experiment. In the case of individual muscles such as the Extensor Indicis and the Extensor Digiti Minimi the belly of the muscle was chosen as the ideal site. In the case of more generalized muscles such as the (1) Flexor Digitorum Superficialis, (2) Flexor Digitorum Profundus, and (3) Extensor Digitorum, palpation was used to determine the area of maximal muscle

movement, and an array of two pairs of sensors were placed over the extensors and an array of three pairs was placed over the flexor group.

Surface contaminants such as dirt, oil, and dead skin were removed using a mildly abrasive cleanser-infused pad to areas where electrodes were placed. Such contaminating materials can impede the travel of bioelectric signals from the skin to the electrodes of the EMG, possibly resulting in erroneously high readings (Schwartz & Andrasik, 2005). Care was taken to avoid irritating the skin.

Once the skin was completely dried, a pair of Grass Technologies model F-E14D pre-gelled disposable Silver/Silver-Chloride (Ag/AgCl) electrodes were placed on each of the seven identified sites using a 20mm center-to-center electrode distance.

In order to validate the effectiveness of the skin preparation, a multimeter was used to test the skin's conductance of electricity. If the resistance between the two electrodes measured greater than 10,000 ohms the sensors were removed and the skin was once again cleaned at that site, allowed to dry, and once again tested for conductance. Care was taken to not irritate the skin. If the second measurement remained greater than 10,000 ohms, the value was noted and the experiment was allowed to continue.

Once the sensor adhesive cured and became secure, seven twisted pairs of Grass Technologies model F-SL reusable snap-ended leads were attached to the electrodes. To minimize pickup of environmental electrical noise, care was taken to keep the leads from each muscle site close together. To minimize crosstalk between signal pairs, care was taken to maintain separation between pairs.

Once all leads were attached to the sensors on the left forearm, the subject was fitted with an 18 sensor CyberTouch instrumented glove onto their left hand.

To reduce forearm pronation/supination, wrist flexion/extension, and thumb movement, a wrist brace was placed over the glove and sensors.

Because the electrical signal present on the skin that is captured by surface EMG sensors is of very high impedance, a Grass Industries High Impedance Input Module was used between the incoming leads and the amplifiers in the EMG, in order to improve the input characteristics of the signals, in accordance with the manufacturer's recommendations.

Positioning of Arm and Calibration of Signals

The following factors were considered important in the placement of the subjects arm:

1. comfort of the subject, maximal relaxation, minimal effort to maintain position
2. isolation of muscle activity (i.e., arm could be maintained in relaxed position without need for muscle activation to maintain position and only muscles in question would be activated in the course of the experimental movements)
3. signal quality/stability
4. clarity of the video recording, including environmental lighting and an unobstructed line of site to the subject's left arm
5. unobstructed motion of the fingers

6. position in which it was possible for the arm to remain stationary for the duration of the data collection

The subject's arm was placed in a position that was comfortable and relaxed, per self-report. Subjects were asked to perform some of the motions that would be required in the experiments and adjustments were made to maximize their ability to maintain that position throughout the course of the experiment.

While the subject was performing these motions the video camera was positioned and sample footage was recorded to assure usefulness.

Once a satisfactory position was found, the EMG and the custom testing software was initialized and the signals were sampled to verify that a clean signal was being recorded. The subject was then asked to perform several of the motions required in the experiment while the signal was recorded and tested for stability, and a determination was made as to whether the setup had successfully isolated the correct muscles (i.e., did not require the use of muscles not being tested).

Adjustments were made until the 6 criteria listed on page 46 were satisfied.

Data collection was initiated and the subject was instructed to relax their hand and arm until the subject's hand and arm were visibly still for a minimum of 30 seconds and signals from the EMG reached a baseline reading. This pause gave the wires a chance to "cool off" long enough to minimize motion artifacts.

For synchronization of the video data, the subject was then asked to quickly clench their fist to provide an easily identifiable marker to facilitate synchronization of the video with the CyberTouch motion data, and, by extension

the EMG data stream. This video synchronization was important for identifying and labeling the exact beginning and end times of each individual finger motion.

First Motion Collection

The first motion collection began with performance of the "motion primitives." Subjects were asked to keep their finger down until instructed to bring their finger back up to the neutral position. Additionally, subjects were reminded to return their finger to the neutral position at the same speed as the down portion of the movement.

Except for the finger being measured for each motion primitive, the subject was instructed to keep as still but relaxed as possible. In this way, movement was localized to the finger being moved. As well, the brace helped to keep the wrist and thumb still and the remaining 3 digits were immobilized manually by holding them. This manual immobilization of the remaining 3 digits was done to allow the subjects to relax without needing to exert any effort to prevent their other 3 digits from moving.

After the collection of motion primitives was completed, the subject was given a chance to rest. During this time, cables and connections were checked. The brace was examined for proper restraint and the arm was checked for unencumbered motion.

During the next phase, subjects were instructed to move their hands as naturally as possible with a great diversity of movements (i.e., to try to avoid repetitive patterns of movement), limited to the four non-thumb digits. The

subject was asked to vary fingers, finger combinations, speed, and vigor/strength of motion. If subjects had difficulty maintaining a varied motion, they were guided by being told activities to pantomime, such as scratching a dog.

Next, the subject was asked to relax the arm for a period of at least 20 seconds, which facilitated the accurate collection of the last portion of the EMG and CyberTouch data.

Second Motion Collection

A second set of quasi-free motion data was collected. The procedure for this data collection was identical to the second half of the first motion collection session.

After the completion of the experiment the subject was asked questions regarding their experience, and was given an opportunity to comment on the experiment itself.

CHAPTER 5

FINDINGS

The following section discusses how data was obtained, describes the data, and presents the results.

Data Collection

The surface EMG sensors were arranged as seven pairs of single-ended electrodes. The two single-ended signals from each pair of electrodes were converted into one differential signal, and amplified to a range of ±2.4V, which (according to documentation provided by National Instruments) is the optimal range for digitization with the NI USB-6009 Multifunction DAQ. These seven signals were combined with the frame sync pulse signal generated by the pulse stretcher from the CyberTouch interface box outputs. All eight signals were then digitized at 2kHz by DAQ1. Seven channels of sEMG data are shown in Figure 7 and represent a capture period of 7 minutes and 20 seconds. The frame pulse is shown in Figure 8. Note that Figure 8 shows only a small subset of the total sampling time in Figure 7 to accurately show the shape of the frame sync pulse.

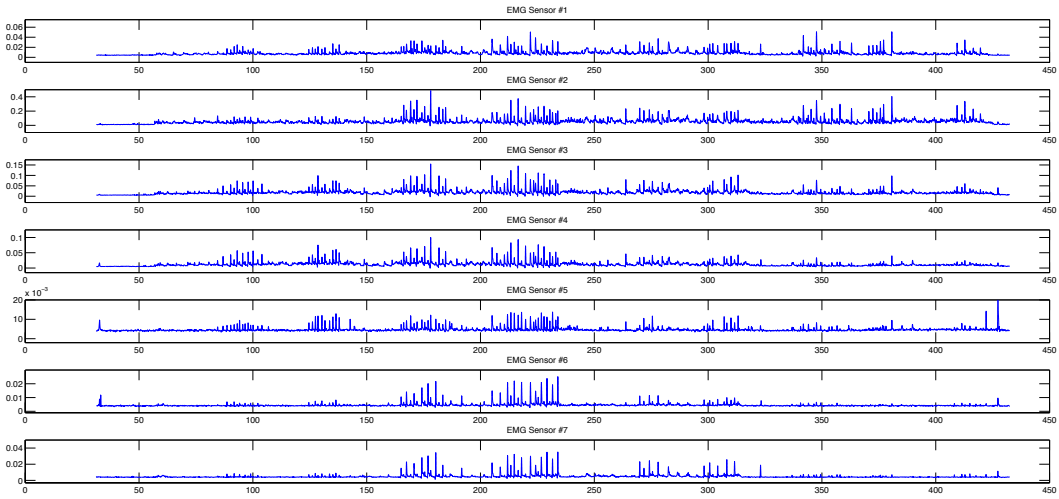

Figure 7. 7 channels of sEMG data captured by DAQ1 (units are in seconds)

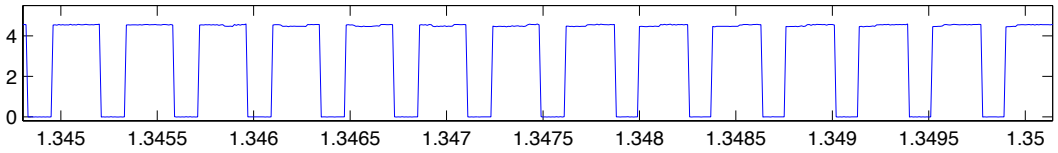

Figure 8. Detail of the frame pulse captured by DAQ1 (units are in seconds)

The raw sync signal generated by the CyberTouch was digitized by DAQ2. This signal was sampled at 48,000 samples per second, and each rising edge of this digitized sync signal represents the exact time that a glove sensor was sampled by the CyberTouch.

Hand posture data collected from the CyberTouch (via custom software) was collected concurrently with the sEMG data (which indicates muscle activation). The 18 CyberTouch signals that collectively represent the moment-by-moment hand posture are shown in Figure 9. The dotted vertical line in Figure 9 marks the boundary between the motion primitive collection phase and the quasi-free motion collection. The value of the motion primitives in isolating individual joint movements is clearly visible.

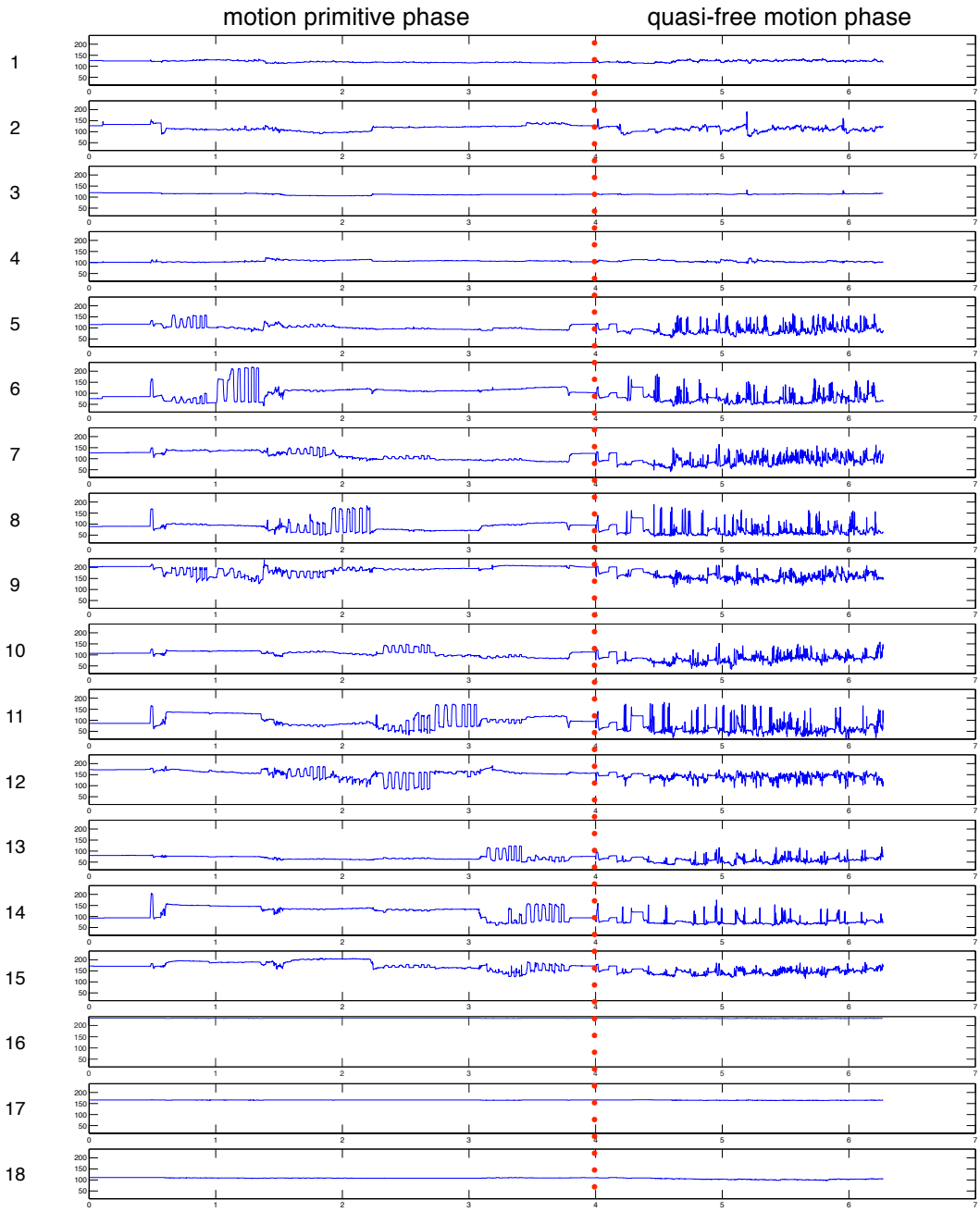

Figure 9. A short experiment to show the hand posture data from all 18 sensors and the difference between the structured script and the free-motion

Data sets such as those shown in Figure 7 and Figure 9 are extremely large. Thus, only this representative sample is included here to show the nature of the results. Complete results will be provided upon request.

Data Processing

Sync pulse signals (see Figure 8) from the CyberTouch interface box were used to synchronize the output data stream from the CyberTouch serial port with the master clock that was used to trigger the sampling of the 7 sEMG signals. Per the CyberTouch documentation, sampling of each glove sensor occurred at the rising edge of a sync pulse, with 18 sync pulses needed to sample all 18 glove sensors. Custom MATLAB code was developed to detect the rising edges of the CyberTouch sync pulses and to construct a table with the exact time that each CyberTouch sample was taken.

The glove data stream, the rising edge time table, and the stretched frame pulse sampled with DAQ1 were combined to produce two tables: one containing the *data* samples collected from the 18 sensors in the CyberTouch glove and the other containing the *time* that each of those samples was taken, according to the master clock that triggered the sampling of the 7 sEMG signals. This entire process is illustrated in Figure 10, with the *data* table and the *timing* table shown at the bottom of Figure 10.

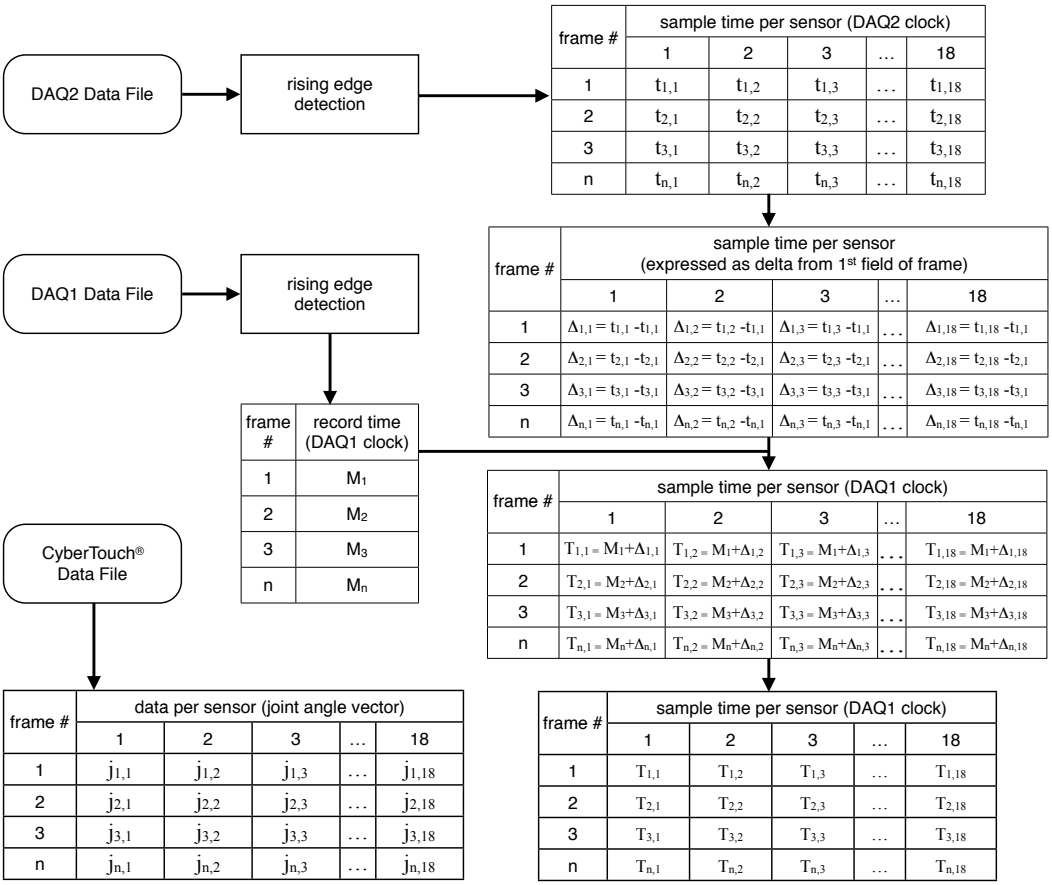

Figure 10. Schematic representation of the process used to synchronize the CyberTouch data stream with the sEMG data stream

As stated in the conceptual framework, the rate and the exact timing of the sampling of the hand posture did not match that of the sEMG signal sampling. However, computation of the correlation between changes in the 18 signals representing the hand posture and changes in the sEMG signals required hand posture samples that were exactly synchronized with the sEMG signals. To provide synchronized hand posture samples interpolated values of the hand posture signals were calculated at each of the sEMG sample times, using cubic interpolation. The result of these calculations was a single table with the time of

every sEMG sample, and an interpolated hand posture data set of 18 samples for exactly that same time. The structure of this table is shown in Table 2.

frame #	time of sEMG sample	interpolated data per sensor (joint angle vector)				
		1	2	3	…	18
1	$t(s)_1$	$i(j)_{1,1}$	$i(j)_{1,2}$	$i(j)_{1,3}$	…	$i(j)_{1,18}$
2	$t(s)_2$	$i(j)_{2,1}$	$i(j)_{2,2}$	$i(j)_{2,3}$	…	$i(j)_{2,18}$
3	$t(s)_3$	$i(j)_{3,1}$	$i(j)_{3,2}$	$i(j)_{3,3}$	…	$i(j)_{3,18}$
n	$t(s)_n$	$i(j)_{n,1}$	$i(j)_{n,2}$	$i(j)_{n,3}$	…	$i(j)_{n,18}$

Table 2. Hand posture interpolation table with a set of 18 hand posture samples to match the time of each sEMG sample

As mentioned in the conceptual framework, it was anticipated that the *acceleration* of the joint rotations (and not the *angle* of the joints) would yield the highest correlation values with the EMG signals. Therefore, velocity and acceleration values were calculated for each joint angle sensor at each sEMG sample time (see Figure 11).

frame #	time of sEMG sample	interpolated data per sensor (joint angle vector)				
		1	2	3	…	18
1	$t(s)_1$	$i(j)_{1,1}$	$i(j)_{1,2}$	$i(j)_{1,3}$	…	$i(j)_{1,18}$
2	$t(s)_2$	$i(j)_{2,1}$	$i(j)_{2,2}$	$i(j)_{2,3}$	…	$i(j)_{2,18}$
3	$t(s)_3$	$i(j)_{3,1}$	$i(j)_{3,2}$	$i(j)_{3,3}$	…	$i(j)_{3,18}$
n	$t(s)_n$	$i(j)_{n,1}$	$i(j)_{n,2}$	$i(j)_{n,3}$	…	$i(j)_{n,18}$

↓

frame #	velocity (v) per sensor				
	1	2	3	…	18
1	N/A	N/A	N/A	…	N/A
2	$(i(j)_{2,1}-i(j)_{1,1})/(t(s)_2-t(s)_1)$	$(i(j)_{2,2}-i(j)_{1,2})/(t(s)_2-t(s)_1)$	$(i(j)_{2,3}-i(j)_{1,3})/(t(s)_2-t(s)_1)$	…	$(i(j)_{2,18}-i(j)_{1,18})/(t(s)_2-t(s)_1)$
3	$(i(j)_{3,1}-i(j)_{2,1})/(t(s)_3-t(s)_2)$	$(i(j)_{3,2}-i(j)_{2,2})/(t(s)_3-t(s)_2)$	$(i(j)_{3,3}-i(j)_{2,3})/(t(s)_3-t(s)_2)$	…	$(i(j)_{3,18}-i(j)_{2,18})/(t(s)_3-t(s)_2)$
n	$(i(j)_{n,1}-i(j)_{n-1,1})/(t(s)_n-t(s)_{n-1})$	$(i(j)_{n,2}-i(j)_{n-1,2})/(t(s)_n-t(s)_{n-1})$	$(i(j)_{n,3}-i(j)_{n-1,3})/(t(s)_n-t(s)_{n-1})$	…	$(i(j)_{n,18}-i(j)_{n-1,18})/(t(s)_n-t(s)_{n-1})$

↓

frame #	acceleration (a) per sensor				
	1	2	3	…	18
1	N/A	N/A	N/A	…	N/A
2	N/A	N/A	N/A		N/A
3	$(v_{3,1}-v_{2,1})/(t(s)_3-t(s)_1)$	$(v_{3,2}-v_{2,2})/(t(s)_3-t(s)_1)$	$(v_{3,3}-v_{2,3})/(t(s)_3-t(s)_1)$	…	$(v_{3,18}-v_{2,18})/(t(s)_3-t(s)_1)$
4	$(v_{4,1}-v_{3,1})/(t(s)_4-t(s)_2)$	$(v_{4,2}-v_{3,2})/(t(s)_4-t(s)_2)$	$(v_{4,3}-v_{3,3})/(t(s)_4-t(s)_2)$	…	$(v_{4,18}-v_{3,18})/(t(s)_4-t(s)_2)$
n	$(v_{n,1}-v_{n-1,1})/(t(s)_n-t(s)_{n-2})$	$(v_{n,2}-v_{n-1,2})/(t(s)_n-t(s)_{n-2})$	$(v_{n,3}-v_{n-1,3})/(t(s)_n-t(s)_{n-2})$	…	$(v_{n,18}-v_{n-1,18})/(t(s)_n-t(s)_{n-2})$

Figure 11: Schematic representation of the process used to convert the 18 joint angles to 18 velocity and 18 acceleration values

The acceleration table in Figure 11 was used to compute the strength of the correlations between joint acceleration and muscle activation, as represented by the sEMG data stream. This computational process will be described in detail later in this chapter.

Synchronization between the video and the EMG sample stream was accomplished by analyzing the motion plots of the subject's hand when they were asked to quickly and completely clench their fist after a 10 second period of complete rest. As shown in Figure 12, the precise beginning of this motion is quite trivial to determine, and the exact time is easily noted. The video taken during the experiment was captured at 60 frames per second. That video footage

was analyzed frame by frame, and the time of the first frame of hand motion (per the video camera's timecode) was noted, and used for synchronization to the master clock.

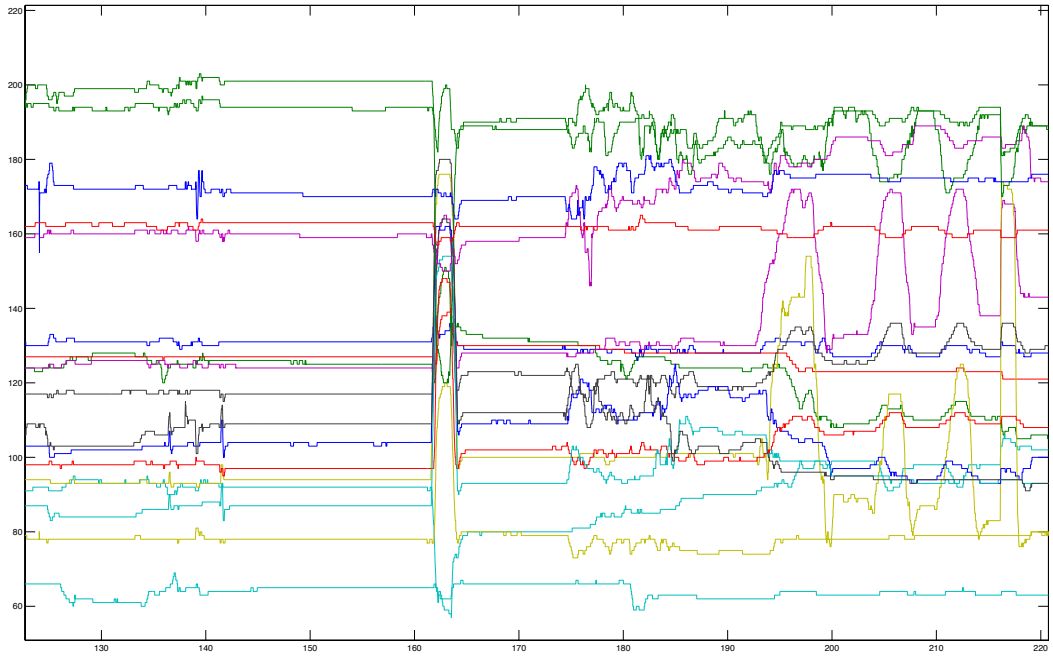

Figure 12: Graph demonstrating the effect of a quick and strong hand-clench on the CyberTouch™ sensors

Once this synchronization point was established, the video footage was analyzed frame by frame to identify the beginning and the end of each of the motion primitives that the subject was asked to perform. The video timecode for each motion primitive was noted. By computing the elapsed time from the synchronization point the timing of any video event can be known, with respect to the master clock.

Table 3 and Table 4 show the worksheets that were used to record the video timecodes, as well as the intermediary calculations that were necessary to synchronize all video events to the master clock.

event	timecode			frames			seconds		
	Δ	start	end	Δ	start	end	Δ	start	end
fist	00:02;15	03:23;16	03:26;18	75	6100	6192	2.5025	203.5369	206.6066
index_PS_1	00:05;04	03:39;02	03:44;05	154	6566	6719	5.1385	219.0858	224.1909
index_PS_2	00:05;21	03:44;06	03:49;26	171	6720	6890	5.7057	224.2242	229.8966
index_PS_3	00:05;03	03:49;27	03:54;29	153	6891	7043	5.1051	229.9299	235.0017
index_PF_1	00:04;15	03:55;00	03:59;14	135	7044	7178	4.5045	235.0350	239.5062
index_PF_2	00:03;28	03:59;15	04:03;14	118	7179	7296	3.9373	239.5395	243.4434
index_PF_3	00:03;27	04:03;15	04:07;11	117	7297	7413	3.9039	243.4768	247.3473
index_SS_1	00:07;13	04:13;14	04:20;26	223	7596	7818	7.4408	253.4535	260.8609
index_SS_2	00:07;24	04:20;27	04:28;20	234	7819	8052	7.8078	260.8942	268.6687
index_SS_3	00:04;21	04:28;21	04:33;11	141	8053	8193	4.7047	268.7020	273.3734
index_SF_1	00:05;07	04:33;12	04:38;18	157	8194	8350	5.2386	273.4067	278.6119
index_SF_2	00:04;19	04:38;19	04:43;07	139	8351	8489	4.6380	278.6453	283.2499
index_SF_3	00:03;09	04:43;08	04:46;16	99	8490	8588	3.3033	283.2833	286.5532
middle_PS_1	00:05;19	05:05;07	05:10;25	169	9147	9315	5.6390	305.2052	310.8108
middle_PS_2	00:06;26	05:10;26	05:17;21	206	9316	9521	6.8735	310.8442	317.6844
middle_PS_3	00:06;03	05:17;22	05:23;24	183	9522	9704	6.1061	317.7177	323.7905
middle_PF_1	00:04;12	05:23;25	05:28;06	132	9705	9836	4.4044	323.8238	328.1949
middle_PF_2	00:04;17	05:28;07	05:32;23	137	9837	9973	4.5712	328.2282	332.7661
middle_PF_3	00:03;19	05:32;24	05:36;12	109	9974	10082	3.6370	332.7995	336.4031
middle_SS_1	00:05;05	05:39;19	05:44;23	155	10179	10333	5.1718	339.6396	344.7781
middle_SS_2	00:05;22	05:44;24	05:50;15	172	10334	10505	5.7391	344.8115	350.5172
middle_SS_3	00:05;06	05:50;16	05:55;21	156	10506	10661	5.2052	350.5506	355.7224
middle_SF_1	00:03;20	05:55;22	05:59;11	110	10662	10771	3.6703	355.7558	359.3927
middle_SF_2	00:05;01	05:59;12	06:04;14	151	10772	10922	5.0384	359.4261	364.4311
middle_SF_3	00:05;21	06:04;15	06:10;05	171	10923	11093	5.7057	364.4645	370.1368
ring_PS_1	00:06;21	06:18;03	06:24;23	201	11331	11531	6.7067	378.0781	384.7514
ring_PS_2	00:05;05	06:24;24	06:29;28	155	11532	11686	5.1718	384.7848	389.9233
ring_PS_3	00:06;18	06:29;29	06:36;16	198	11687	11884	6.6066	389.9566	396.5299
ring_PF_1	00:03;16	06:36;17	06:40;02	106	11885	11990	3.5369	396.5632	400.0667
ring_PF_2	00:03;13	06:47;11	06:50;23	103	12209	12311	3.4368	407.3740	410.7774
ring_PF_3	00:04;16	06:50;24	06:55;09	136	12312	12447	4.5379	410.8108	415.3153
ring_SS_1	00:05;13	06:57;10	07:02;24	163	12508	12670	5.4388	417.3507	422.7561
ring_SS_2	00:06;24	07:02;25	07:09;18	204	12671	12874	6.8068	422.7895	429.5629
ring_SS_3	00:06;02	07:09;19	07:15;20	182	12875	13056	6.0727	429.5963	435.6356
ring_SF_1	00:06;11	07:15;21	07:22;01	191	13057	13247	6.3730	435.6690	442.0087
ring_SF_2	00:04;08	07:22;02	07:26;09	128	13248	13375	4.2709	442.0420	446.2796
ring_SF_3	00:04;01	07:26;10	07:30;10	121	13376	13496	4.0374	446.3130	450.3170
pinkie_PS_1	00:04;24	07:36;18	07:41;11	144	13684	13827	4.8048	456.5899	461.3614
pinkie_PS_2	00:05;13	07:41;12	07:46;24	163	13828	13990	5.4388	461.3947	466.8001
pinkie_PS_3	00:05;21	07:46;25	07:52;15	171	13991	14161	5.7057	466.8335	472.5058
pinkie_PF_1	00:03;23	07:52;16	07:56;08	113	14162	14274	3.7704	472.5392	476.2763
pinkie_PF_2	00:03;25	07:56;09	08:00;05	115	14275	14389	3.8372	476.3096	480.1134
pinkie_PF_3	00:03;27	08:00;06	08:04;02	117	14390	14506	3.9039	480.1468	484.0174
pinkie_SS_1	00:05;06	08:06;29	08:12;04	156	14593	14748	5.2052	486.9203	492.0921
pinkie_SS_2	00:05;18	08:12;05	08:17;22	168	14749	14916	5.6056	492.1255	497.6977
pinkie_SS_3	00:06;04	08:17;23	08:23;26	184	14917	15100	6.1395	497.7311	503.8372
pinkie_SF_1	00:03;19	08:23;27	08:27;15	109	15101	15209	3.6370	503.8705	507.4741
pinkie_SF_2	00:05;15	08:27;16	08:33;00	165	15210	15374	5.5055	507.5075	512.9796
pinkie_SF_3	00:03;18	08:33;01	08:36;18	108	15375	15482	3.6036	513.0130	516.5832

Table 3. Worksheet for converting video timecode to seconds (decimal values for seconds have been rounded to 4 decimal places for display in this table)

event	seconds (from sync point)			seconds (on *master clock*)		
	Δ	start	end	Δ	start	end
fist	2.5025	0.0000	3.0697	2.5025	47.7000	50.7697
index_PS_1	5.1385	15.5489	20.6540	5.1385	63.2489	68.3540
index_PS_2	5.7057	20.6874	26.3597	5.7057	68.3874	74.0597
index_PS_3	5.1051	26.3931	31.4648	5.1051	74.0931	79.1648
index_PF_1	4.5045	31.4982	35.9693	4.5045	79.1982	83.6693
index_PF_2	3.9373	36.0027	39.9066	3.9373	83.7027	87.6066
index_PF_3	3.9039	39.9399	43.8105	3.9039	87.6399	91.5105
index_SS_1	7.4408	49.9166	57.3240	7.4408	97.6166	105.0240
index_SS_2	7.8078	57.3574	65.1318	7.8078	105.0574	112.8318
index_SS_3	4.7047	65.1652	69.8365	4.7047	112.8652	117.5365
index_SF_1	5.2386	69.8699	75.0751	5.2386	117.5699	122.7751
index_SF_2	4.6380	75.1084	79.7130	4.6380	122.8084	127.4130
index_SF_3	3.3033	79.7464	83.0163	3.3033	127.4464	130.7163
middle_PS_1	5.6390	101.6683	107.2739	5.6390	149.3683	154.9739
middle_PS_2	6.8735	107.3073	114.1475	6.8735	155.0073	161.8475
middle_PS_3	6.1061	114.1808	120.2536	6.1061	161.8808	167.9536
middle_PF_1	4.4044	120.2870	124.6580	4.4044	167.9870	172.3580
middle_PF_2	4.5712	124.6914	129.2292	4.5712	172.3914	176.9292
middle_PF_3	3.6370	129.2626	132.8662	3.6370	176.9626	180.5662
middle_SS_1	5.1718	136.1028	141.2412	5.1718	183.8028	188.9412
middle_SS_2	5.7391	141.2746	146.9803	5.7391	188.9746	194.6803
middle_SS_3	5.2052	147.0137	152.1855	5.2052	194.7137	199.8855
middle_SF_1	3.6703	152.2189	155.8559	3.6703	199.9189	203.5559
middle_SF_2	5.0384	155.8892	160.8942	5.0384	203.5892	208.5942
middle_SF_3	5.7057	160.9276	166.5999	5.7057	208.6276	214.2999
ring_PS_1	6.7067	174.5412	181.2145	6.7067	222.2412	228.9145
ring_PS_2	5.1718	181.2479	186.3864	5.1718	228.9479	234.0864
ring_PS_3	6.6066	186.4198	192.9930	6.6066	234.1198	240.6930
ring_PF_1	3.5369	193.0264	196.5299	3.5369	240.7264	244.2299
ring_PF_2	3.4368	203.8372	207.2406	3.4368	251.5372	254.9406
ring_PF_3	4.5379	207.2739	211.7784	4.5379	254.9739	259.4784
ring_SS_1	5.4388	213.8138	219.2192	5.4388	261.5138	266.9192
ring_SS_2	6.8068	219.2526	226.0260	6.8068	266.9526	273.7260
ring_SS_3	6.0727	226.0594	232.0988	6.0727	273.7594	279.7988
ring_SF_1	6.3730	232.1321	238.4718	6.3730	279.8321	286.1718
ring_SF_2	4.2709	238.5052	242.7427	4.2709	286.2052	290.4427
ring_SF_3	4.0374	242.7761	246.7801	4.0374	290.4761	294.4801
pinkie_PS_1	4.8048	253.0531	257.8245	4.8048	300.7531	305.5245
pinkie_PS_2	5.4388	257.8579	263.2633	5.4388	305.5579	310.9633
pinkie_PS_3	5.7057	263.2966	268.9690	5.7057	310.9966	316.6690
pinkie_PF_1	3.7704	269.0023	272.7394	3.7704	316.7023	320.4394
pinkie_PF_2	3.8372	272.7728	276.5766	3.8372	320.4728	324.2766
pinkie_PF_3	3.9039	276.6099	280.4805	3.9039	324.3099	328.1805
pinkie_SS_1	5.2052	283.3834	288.5552	5.2052	331.0834	336.2552
pinkie_SS_2	5.6056	288.5886	294.1608	5.6056	336.2886	341.8608
pinkie_SS_3	6.1395	294.1942	300.3003	6.1395	341.8942	348.0003
pinkie_SF_1	3.6370	300.3337	303.9373	3.6370	348.0337	351.6373
pinkie_SF_2	5.5055	303.9706	309.4428	5.5055	351.6706	357.1428
pinkie_SF_3	3.6036	309.4761	313.0464	3.6036	357.1761	360.7464

Table 4. Worksheet for synchronizing the video timecode (converted to seconds in Table 3) to the *master clock*

Results

Finding Correlation

Now that the raw hand posture data is represented as the acceleration of each joint when each sEMG sample was taken, it is possible to determine the extent to which these two data streams are correlated to each other. Correlation is a dimensionless value that represents the degree of similarity between two sets of random variables. The magnitude of this similarity is expressed as a *correlation coefficient*, which represents the degree to which one can expect changes in one signal to occur simultaneously with changes in the other signal.

To determine the extent to which the posture changes of the hand and the surface electromyographic signals are correlated, the Pearson Product-Moment Correlation Coefficient was calculated for each of the seven sEMG sensors with respect to each of the 18 CyberTouch joint-angle sensors. Examples of the results of these calculations are presented in Table 5 and Table 6. The numerical values in each cell of this table represent the strength of the correlation between one hand posture sample stream and one sEMG sample stream. The purpose of this table is to show which joint-angle rotations are correlated with which muscle activations, as indicated by the sEMG sample streams. The qualitative strength of each correlation can be expressed as a function of the numerical correlation coefficient as shown in Table 7 (Cohen, 1988). Based on these, it is possible to describe the relationship between these signals in terms of

the extent to which changes in one signal could be expected to correlate with changes in the other.

Results of the correlation calculations for the middle finger *scratch fast* motion primitive are shown in Table 5 (for the "down" portion of the movement) and Table 6 (for the "up" portion of the movement). The complete results for each subject produced 32 sets of these 7x18 tables.

Glove Sensors	sEMG Sensors						
	1	2	3	4	5	6	7
1	0.5021	0.5770	0.5941	0.5973	0.5701	0.5643	0.5595
2	0.5659	0.7488	0.7385	0.7426	0.5443	0.5352	0.5487
3	0.4571	0.6061	0.6137	0.6123	0.4305	0.4168	0.4304
4	0.6167	0.6137	0.5983	0.6029	0.6492	0.6465	0.6388
5	0.6038	0.4681	0.4767	0.4839	0.5562	0.6939	0.7335
6	0.5358	0.6002	0.6221	0.6189	0.5479	0.5416	0.5358
7	0.6967	0.5011	0.4784	0.4811	0.5802	0.7440	0.7930
8	0.7241	0.4878	0.4833	0.4911	0.5689	0.7376	0.7867
9	0.5533	0.6810	0.6812	0.6870	0.5142	0.5475	0.5668
10	0.6335	0.6662	0.6510	0.6406	0.6378	0.7021	0.7211
11	0.4954	0.5334	0.5255	0.5325	0.5255	0.5395	0.5329
12	0.7118	0.5085	0.4891	0.4722	0.5824	0.7456	0.7904
13	0.6361	0.7320	0.7136	0.7082	0.6452	0.6720	0.6855
14	0.7827	0.7945	0.7950	0.7890	0.7581	0.7445	0.7406
15	0.5892	0.7667	0.7684	0.7611	0.5746	0.5289	0.5331
16	0.5485	0.5959	0.6192	0.6274	0.5818	0.5613	0.5477
17	0.4704	0.6824	0.6848	0.6888	0.5062	0.5230	0.5207
18	0.4900	0.6738	0.6600	0.6615	0.4739	0.4808	0.5019

Table 5. Numerical Pearson Product Moment Correlation Coefficient values for middle finger fast scratch down

Glove Sensors	sEMG Sensors						
	1	2	3	4	5	6	7
1	0.6209	0.6872	0.6956	0.6927	0.6051	0.5880	0.5892
2	0.7053	0.5266	0.5284	0.5130	0.5701	0.7018	0.7394
3	0.3979	0.4112	0.4317	0.4302	0.3635	0.3993	0.4119
4	0.6272	0.5589	0.5259	0.5087	0.5377	0.6687	0.7197
5	0.5146	0.7278	0.7259	0.7287	0.5253	0.5194	0.5237
6	0.5913	0.4641	0.4582	0.4625	0.5475	0.6600	0.6930
7	0.5252	0.7179	0.7200	0.7237	0.5160	0.5256	0.5362
8	0.5416	0.7359	0.7326	0.7374	0.5180	0.5399	0.5474
9	0.7218	0.5009	0.4851	0.4663	0.5707	0.7431	0.7950
10	0.7215	0.7584	0.7614	0.7590	0.7489	0.7218	0.7028
11	0.5607	0.6709	0.6367	0.6317	0.5442	0.5551	0.5813
12	0.5186	0.6850	0.6884	0.6928	0.4964	0.5181	0.5380
13	0.6589	0.6224	0.6277	0.6236	0.6435	0.6334	0.6139
14	0.5698	0.7998	0.7982	0.7918	0.5920	0.5357	0.5484
15	0.6124	0.5268	0.5313	0.5301	0.5571	0.5826	0.5776
16	0.6322	0.5237	0.4831	0.4721	0.5611	0.6820	0.7184
17	0.6989	0.4731	0.4823	0.4687	0.5542	0.7112	0.7623
18	0.5807	0.4847	0.4961	0.4982	0.5027	0.5791	0.5998

Table 6. Numerical Pearson Product Moment Correlation Coefficient values for middle finger fast scratch up

Correlation Category	Correlation Coefficient Value
None	0.0 – 0.09
Small	0.1 – 0.3
Medium	0.3 – 0.5
Strong	0.5 – 1.0

Table 7. Qualitative descriptors of correlation strength for Pearson Product Moment Correlation Coefficient (Cohen, 1988)

Purpose

As mentioned earlier, past attempts to ascertain the health of the individual muscles of the forearm from surface EMG signals alone have been unsatisfactory. This is because it is difficult to extract the signal from the muscle of interest from the cacophony of signals from other muscles in the forearm, which are also picked up by the surface EMG electrodes. In order to sort out all of these combined muscle activation signals, independently derived signals need to be

simultaneously sampled. We need to simultaneously sample signals that are highly correlated to the activation level of each independent muscle.

To provide a familiar example of this approach to signal extraction, imagine that your task is to understand what is being spoken by one person in an audio recording of 15 people speaking simultaneously. The end result is a muddled cacophony, making it extraordinarily difficult to make out what is being said by the person of interest over the din.

However, this task is made substantially easier if you are also given a video recording of the target speaker's mouth. This is because the two data sources (i.e., the audio and the video) are derived from the same phenomenon, and the video signal provides a data stream that can be mentally correlated with the audio signal. The voice signal of interest is the one that is best correlated with the lip and mouth movements in the video. In contrast, if this video only showed the hands of the speaker, there might not be enough of a correlation between the two data streams to allow reliable extraction of the voice of interest from the blended voices.

The goal of this experiment is to quantitatively demonstrate that hand posture data derived from a CyberTouch glove can provide independent signal streams that have a high enough correlation with individual muscle activations in the forearm to separate the individual muscle signals form each other, despite their mixture in the surface EMG signals.

The correlation coefficients shown in the 18x7 format of Table 5 and Table 6 represent a distillation of tens of millions of individual data points.

However, even with this summary, it is difficult to draw general inferences. To facilitate the process of interpretation, the numerical correlation coefficient values in these tables are converted to a gray scale representation, where black is used to show a correlation of zero and white is used to show a perfect correlation of one. Intermediate correlation values between zero and one are represented by intermediate levels of gray. Figure 13 shows the result of this conversion for the data shown in Table 5 and Table 6.

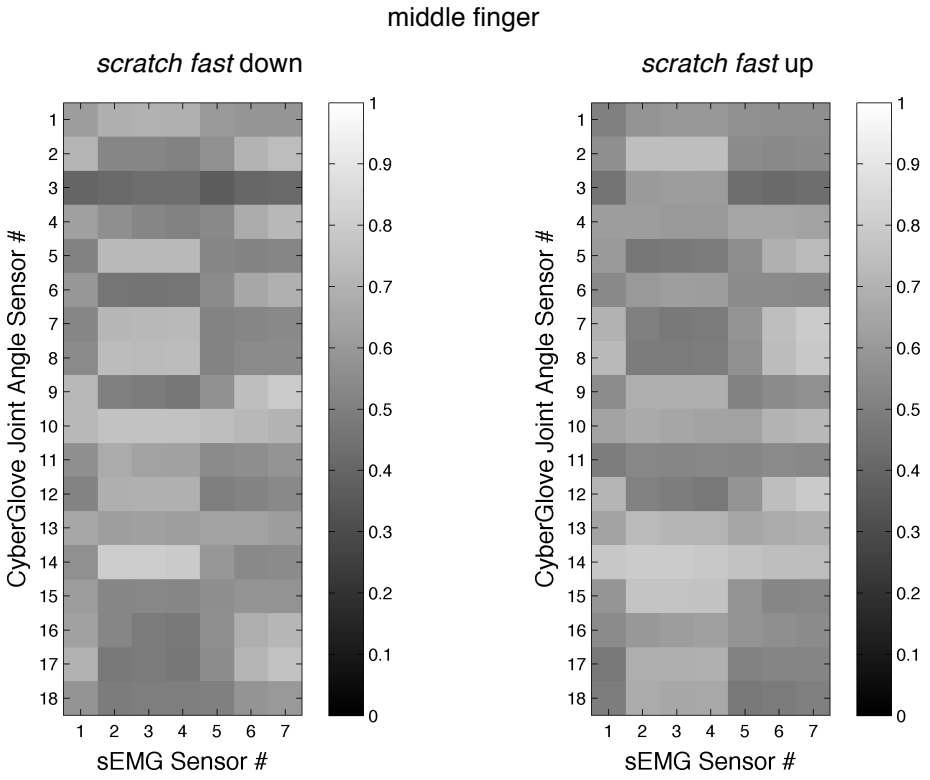

Figure 13. Gray scale representation of correlation coefficient values for middle finger scratch fast motion primitives

Hypotheses regarding the use of slow vs. fast motions

Hypothesis 1

The 16 motion primitives were performed with both quick and slow finger movement. Because the quick finger movement produces larger acceleration values, and because increased muscle force would be required for such a movement, I hypothesized that when the subjects performed the finger motion primitives as fast as they could, this would result in larger correlation values.

Hypothesis 2

Because the slow finger movement produces smaller acceleration values, and because less muscle force would be required for such a movement, I hypothesized that when subjects performed the finger motion primitives slowly, this would result in smaller correlation values. Additionally, due to the non-stationary nature of the electromyographic signal, a slow movement would likely require multiple low-amplitude muscle firings (characterized by repeated amplitude peaks and valleys) to complete the finger movement. Since the finger motion would be largely continuous, the alternation in the sEMG signal would likely produce lower correlation between the two data streams.

Hypothesis 3

Finally, I hypothesized that quick movement should result in a greater distinction between the flexor/extensor antagonist pairs because, as the joint was (ostensibly) rotating at maximum velocity, there would be less need to counteract the motion by the antagonist muscles to reduce the velocity of the joint's movement.

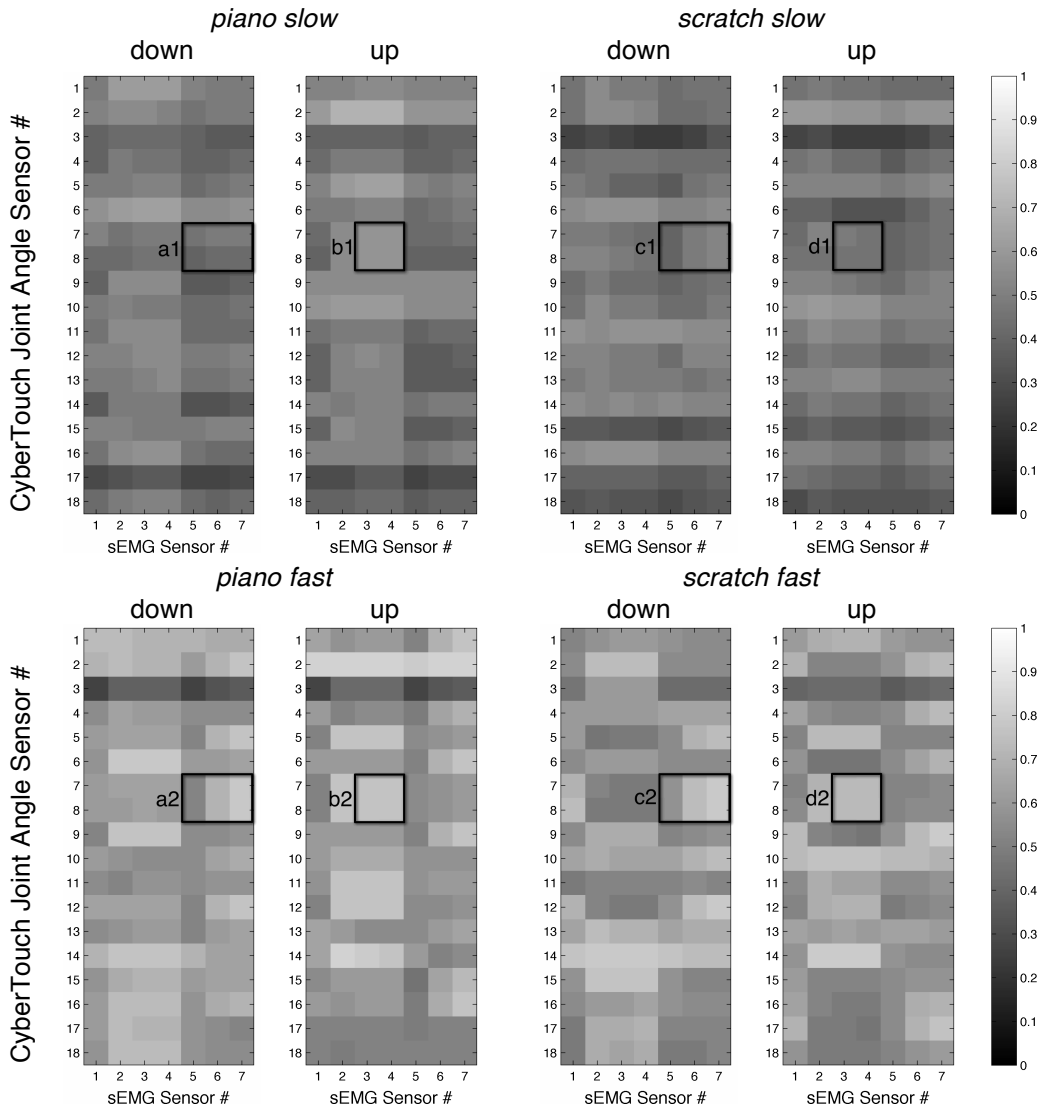

Figure 14. Correlation matrices for fast and slow middle finger motion primitives

Figure 14 shows the gray scale converted correlation matrices for both the fast and slow motion primitives for the middle finger. Overall, the larger correlation values for the fast motion primitives are immediately evident. It is when we look at the areas of predicted interest that we can see the extent of the increase in correlation values for fast finger movement when compared to the same region in the matrices showing the correlation values for the slow finger

movement. The areas of immediate interest for the middle finger motion primitives are highlighted in Figure 14.

The areas labeled a1 and a2 in Figure 14 show the correlation values of the movement of the (1) metacarpophalangeal (MPJ) and (2) proximal interphalangeal (PIJ) joints of the *middle finger* (sampled by the 7th and 8th sensors of the CyberTouch glove) when calculated with respect to the muscle activations of the Flexor Digitorum Superficialis and the Flexor Digitorum Profundus—responsible for the *flexion* of the *middle finger* at the MPJ and the PIJ, respectively—sampled by the 5th, 6th, and 7th sEMG electrodes. The area of interest for the slow *piano down* motion primitive, labeled a1, has an average correlation value of 0.447. The same area for the fast *piano down* motion primitive, labeled a2, has an average correlation value of 0.672, or a 50.34% larger correlation value than the same motion performed slowly. This is in agreement with Hypothesis 1.

The areas labeled b1 and b2 in Figure 14 show the correlation values of the movement of the (1) metacarpophalangeal (MPJ) and (2) proximal interphalangeal (PIJ) joints of the *middle finger* (sampled by the 7th and 8th sensors of the CyberTouch glove) when calculated with respect to the muscle activations of the Extensor Digitorum—responsible for the *extension* of the *middle finger*—sampled by the 3rd and 4th sEMG electrodes. The area of interest for the slow *piano up* motion primitive, labeled b1, has an average correlation value of 0.583. The same area for the fast *piano up* motion primitive, labeled b2, has an average correlation value of 0.771, or a 32.25% larger correlation value

than the same motion performed slowly. Again, this is in agreement with Hypothesis 1.

The areas labeled c1 and c2 in Figure 14 show the correlation values of the movement of the (1) metacarpophalangeal (MPJ) and (2) proximal interphalangeal (PIJ) joints of the *middle finger* (sampled by the 7th and 8th sensors of the CyberTouch glove) when calculated with respect to the muscle activations of the Flexor Digitorum Superficialis and the Flexor Digitorum Profundus—responsible for the *flexion* of the *middle finger* at the MPJ and the PIJ, respectively—sampled by the 5th, 6th, and 7th sEMG electrodes. The area of interest for the slow *scratch down* motion primitive, labeled c1, has an average correlation value of 0.463. The same area for the fast *scratch down* motion primitive, labeled c2, has an average correlation value of 0.702, or a 51.62% larger correlation value than the same motion performed slowly. Again, this is in agreement with Hypothesis 1.

The areas labeled d1 and d2 in Figure 14 show the correlation values of the movement of the (1) metacarpophalangeal (MPJ) and (2) proximal interphalangeal (PIJ) joints of the *middle finger* (sampled by the 7th and 8th sensors of the CyberTouch glove) when calculated with respect to the muscle activations of the Extensor Digitorum—responsible for the *extension* of the *middle finger*—sampled by the 3rd and 4th sEMG electrodes. The area of interest for the slow *scratch up* motion primitive, labeled d1, has an average correlation value of 0.459. The same area for the fast *piano up* motion primitive, labeled d2, has an average correlation value of 0.728, or a 58.61% larger correlation value

than the same motion performed slowly. Again, this is in agreement with Hypothesis 1.

General impressions from the data taken as a whole

Figure 16 shows the Pearson Product-Moment Correlation Coefficient matrices for all fast motion primitives performed for a single participant. Although I will go into detailed analysis of the results for each finger motion later in this chapter, it possible to glean an overall impression of whether the two data streams are related to each other. If the signals from the sEMG sensors and the CyberTouch's positions sensors were entirely uncorrelated, all of the cells in the matrices would be black or nearly black, with no patterns in the distributions of higher vs. lower areas of correlation, as shown in the example correlation matrix in Figure 15.

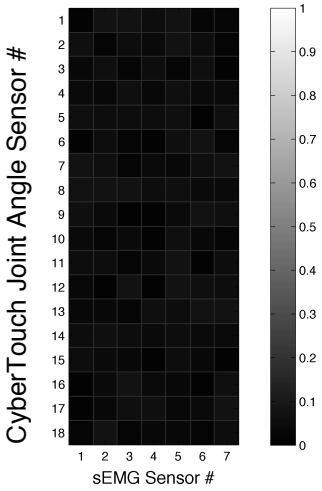

Figure 15. Example of a correlation matrix for totally uncorrelated data streams

However, Figure 16 shows, at a cursory level, that the two sets of signals are correlated to greater or lesser degrees, warranting a more in-depth analysis of the correlations between particular EMG signals and individual finger motions.

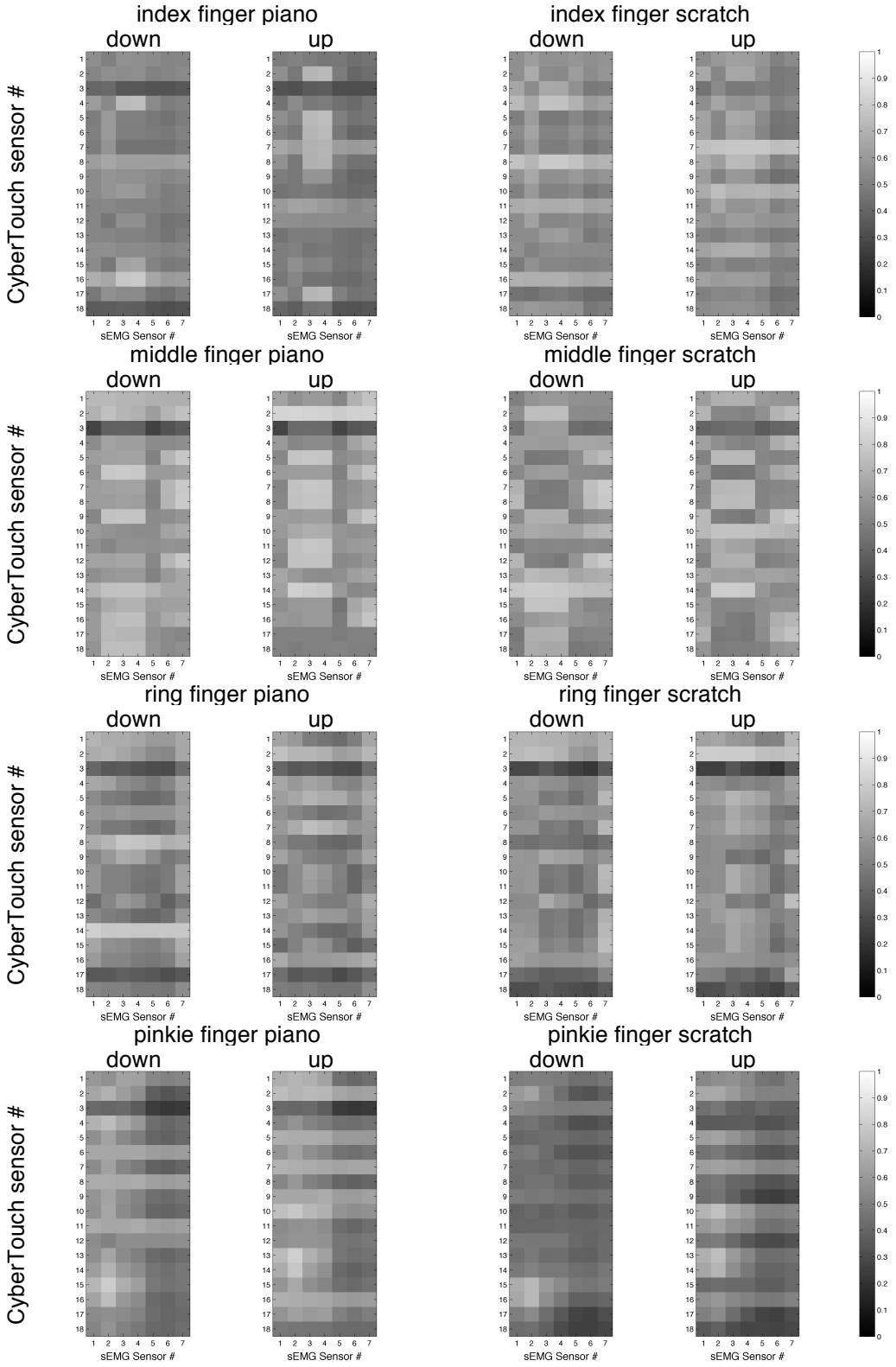

Figure 16. Gray scale representation of correlation coefficients for the fast motion primitives of all four fingers

Before proceeding onto the analysis of the individual finger motion primitives it would be useful to identify the joint angle sensors that are used to capture the motion of each of the subjects' fingers. Additionally, I will describe the biomechanical interconnections between the forearm muscles and their finger motions, and present my rationale for where the sEMG sensors were placed on the forearm. This will allow correlations to be predicted prior to running the experiment, and will provide a basis for evaluating the results.

As described in Chapter 4, hand posture data was captured for the four non-thumb digits. Figure 17 shows the locations of the eight relevant sensors for measuring the movement of these fingers. Table 8 contains descriptions of the joints where the sensors are located. Each of the four fingers contains two joint angle sensors: (1) at the joint where the finger meets the palm, or the metacarpophalangeal joint (MPJ) and (2) at the second joint, or the proximal interphalangeal joint (PIJ). The two (*piano down* and *scratch down*) motion primitives were designed to maximize the use of each of these joints, as distinct muscles control their flexion. The Flexor Digitorum Superficialis (shown in Figure 18) activates the flexion of the MPJ, whose movement is maximized in the *piano down* motion primitive. Flexion of the PIJ, whose movement is maximized in the *scratch down* motion primitive, is controlled by the Flexor Digitorum Profundus (shown in Figure 19) located directly beneath the Flexor Digitorum Superficialis. The tendons of these two muscles connect to the finger as shown in Figure 20.

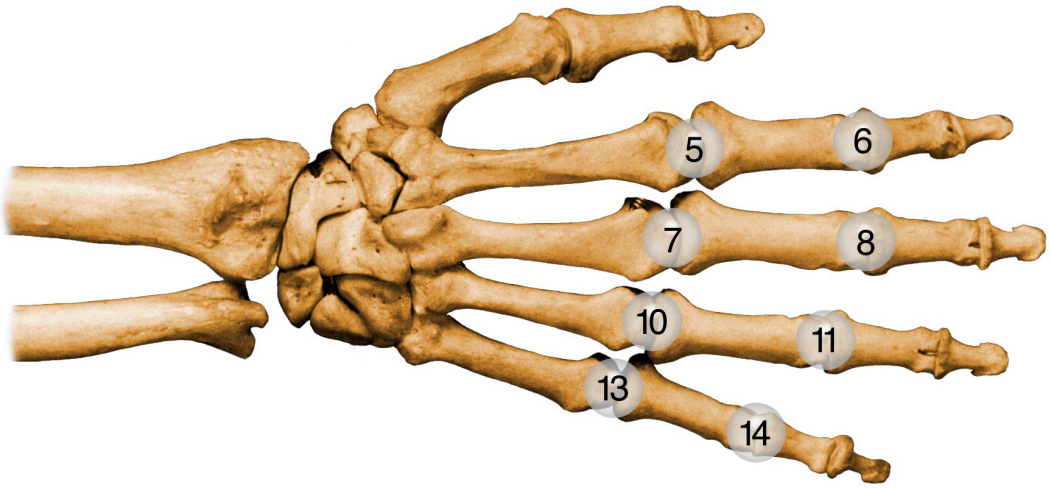

Figure 17. Locations of significant CyberTouch joint angle sensors

Sensor #	Sensor Name (Description)
5	index MPJ (joint where the index meets the palm)
6	index PIJ (joint second from finger tip)
7	middle MPJ (joint where the middle finger meets the palm)
8	middle PIJ (joint second from finger tip of the middle finger)
10	(joint where the ring finger meets the palm)
11	ring PIJ (joint second from finger tip of the ring finger)
13	pinkie MPJ (joint where the pinkie finger meets the palm)
14	pinkie PIJ (joint second from finger tip of the pinkie finger)

Table 8. Descriptions of significant CyberTouch joint angle sensors

Figure 18. Flexor Digitorum Superficialis

Figure 19. Flexor Digitorum Profundus

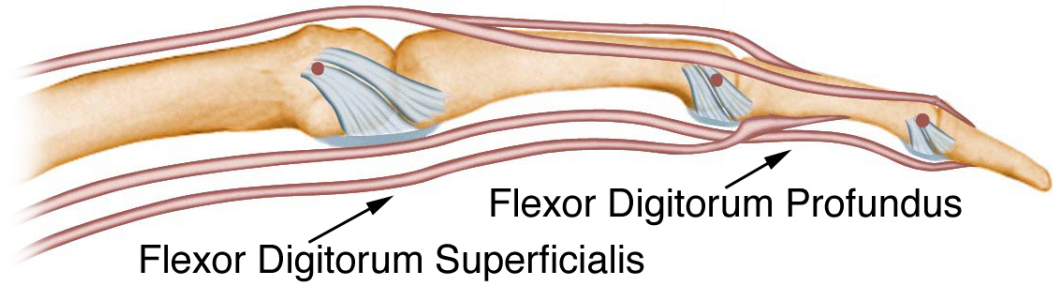

Figure 20. Insertion of the tendons from muscles controlling flexion of the fingers

Figure 21. Extensor Digitorum

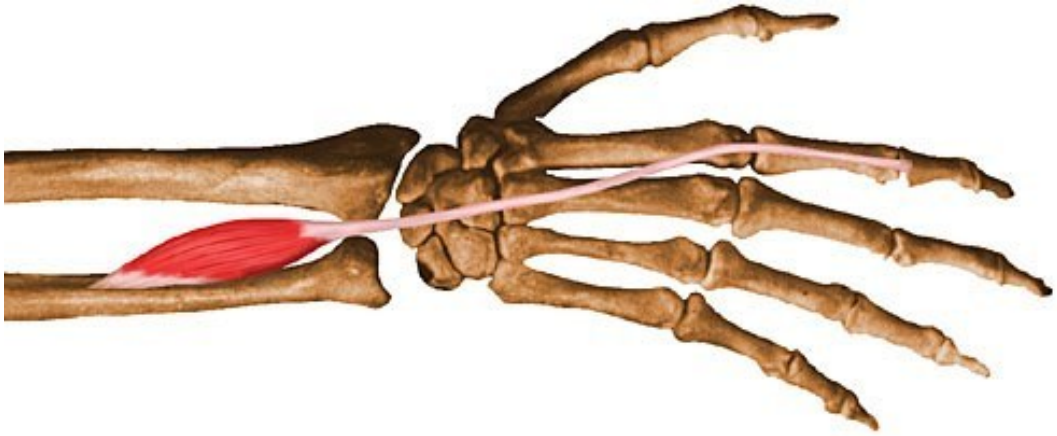

Figure 22. Extensor Indicis

Figure 23. Extensor Digiti Minimi

Extension of all four digits is controlled by the Extensor Digitorum (shown in Figure 21). Additionally, the index finger and the pinkie finger have supplemental, dedicated extensors: the Extensor Indicis (shown in Figure 22) and the Extensor Digiti Minimi (shown in Figure 23), respectively.

Figure 24 shows where the sEMG sensors were placed on the subject's arm. Sensors 5, 6, and 7 (located on the anterior portion of the arm) were arranged as an array, to detect the electromyographic signals generated by the Flexor Digitorum Profundus and the Flexor Digitorum Superficialis, which activate *flexion* of the fingers. Sensors 3 and 4 (located on the posterior of the subject's arm) were arranged as an array to detect the signals generated by the Extensor Digitorum, which activates the extension of all four fingers. Sensor 2 was placed directly above the belly of the Extensor Digiti Minimi (pinkie finger extension, see Figure 23). Sensor 1 was placed directly above the belly of the Extensor Indicis (index finger extension, see Figure 22).

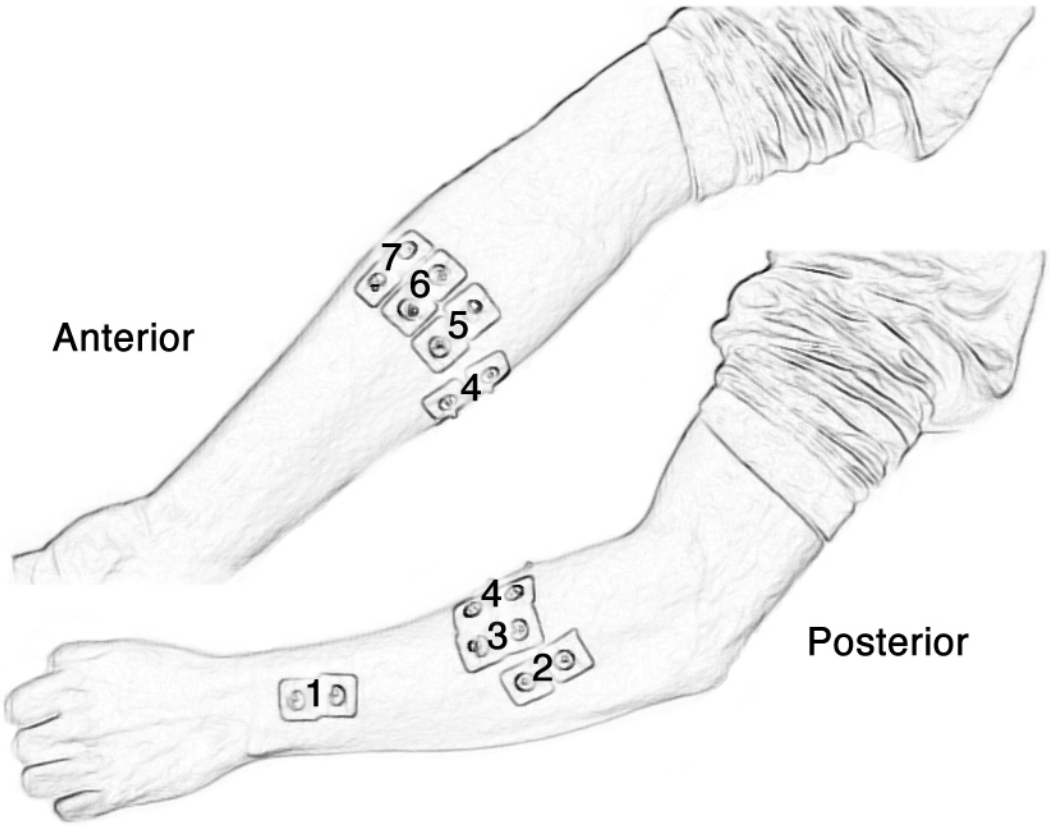

Figure 24. Location of sEMG sensors on the subject's arm

The biomechanical linkages between the forearm muscles and the various digits provide a basis for the hypotheses that underpinned the design of the experiment, and the rationale for the predictions that were made for the results of the data collection. What follows is a more detailed examination of the results for each finger. I will begin by enumerating the biomechanical linkages for each of the motion primitives. Then, I will show my predictions regarding where high correlation values should be found, based on this knowledge. A set of mocked-up correlation matrices will help to show the areas of interest, and will help to compare the results of the experiment with the predictions of the hypotheses.

2nd Digit (index finger)

Two motion primitives were analyzed for the index finger: *piano fast* and *scratch fast*. Figure 25 shows the areas of interest where my hypothesis predicts elevated correlation values.

Motion capture for the *piano fast* motion primitive was primarily sampled by CyberTouch joint angle sensor number 5, although some movement would be impossible to avoid in the PIJ (middle knuckle), sampled by sensor 6. The downward movement (flexion) of the finger at the MPJ is controlled by the Flexor Digitorum Superficialis (sEMG sensors 5, 6, and 7), while the upward motion (extension) is controlled by the Extensor Digitorum (sEMG sensors 3 and 4) and, to a lesser degree, the Extensor Indicis (sEMG sensor 1).

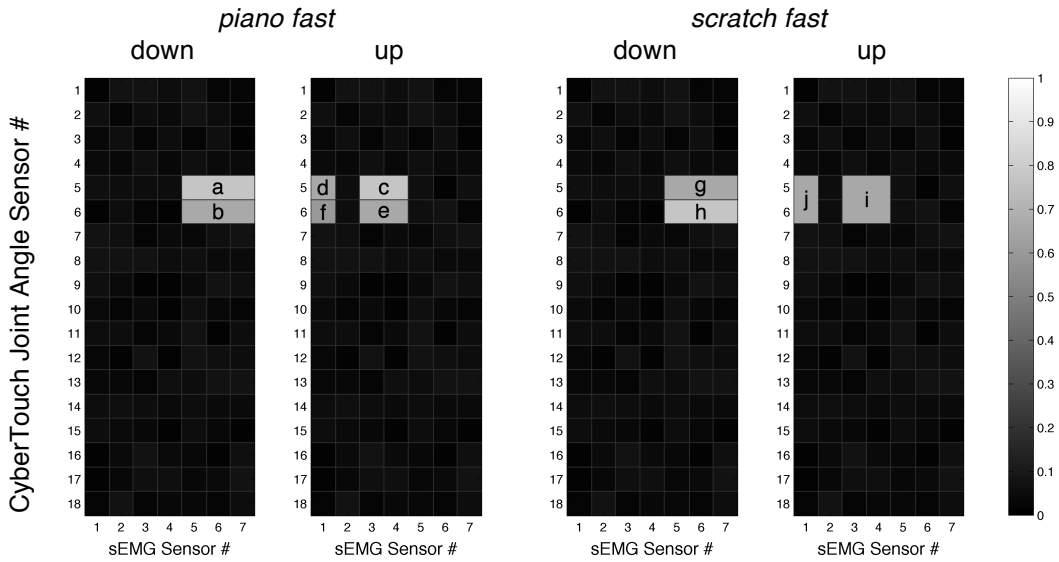

Figure 25. Predicted areas of high correlation for fast piano and scratch motion primitives for the index finger based on biomechanical linkages

During flexion, one would expect to see higher correlations in the region labeled a in Figure 25 (the area including (5,5), (5,5), and (7,5)), and (to a lesser extent) due to inadvertent movement of the PIJ, some higher correlation values in the region labeled b (the area including (5,6), (6,6), and (7,6)). Alternatively, during extension, one would expect to see higher correlation in the region labeled c (the area including (3,5) and (4,5)), and, due to slight contribution form the Extensor Indicis, higher correlation values in the region labeled d (cell (1,5)). Also, as was the case for flexion, inadvertent movement of the PIJ could result in higher correlation values in the region labeled e (the area including (3,6) and (4,6)) as Hypothesis 3 predicts some degree of *alternation* in the aforementioned regions between the flexion and extension portions of the motion primitive, such that the lighter areas of higher correlation for flexion should be markedly darker for extension, and vice versa.

Motion capture for the *scratch fast* motion primitive was sampled by CyberTouch joint angle sensors 5 and 6. The downward movement (flexion) of the finger at the PIJ is controlled by the Flexor Digitorum Profundus and at the MPJ by the Flexor Digitorum Superficialis (sEMG sensors 5, 6, and 7), while the upward motion (extension) is controlled by the Extensor Digitorum (sEMG sensors 3 and 4) and, to a greater degree than for the *piano fast* motion primitive, the Extensor Indicis (sEMG sensor 1).

As such, during flexion, one would expect to see higher correlation in the regions labeled g and h (the area including (5,5), (6,6), and (7,6)). Due to a greater degree of movement for the PIJ than the MPJ in this motion primitive, correlation should be slightly higher in the region labeled h (the area including (5,6), (6,6), and (7,6)) than the region labeled g (the area including (5,5), (6,5), and (7,5)). Alternatively, during extension, one would expect to see increased correlation in the region labeled i (the area including (3,5), (4,5), (3,6), and (4,6)) with a roughly similar correlation value for the region labeled j (the area including (1,5) and (1,6)), due to the significant contribution form the Extensor Indicis.

Hypothesis 3 predicts some degree of *alternation* in the aforementioned regions between the flexion and extension portions of the motion primitive, such that the lighter areas of higher correlation for flexion should be markedly darker for extension, and vice versa.

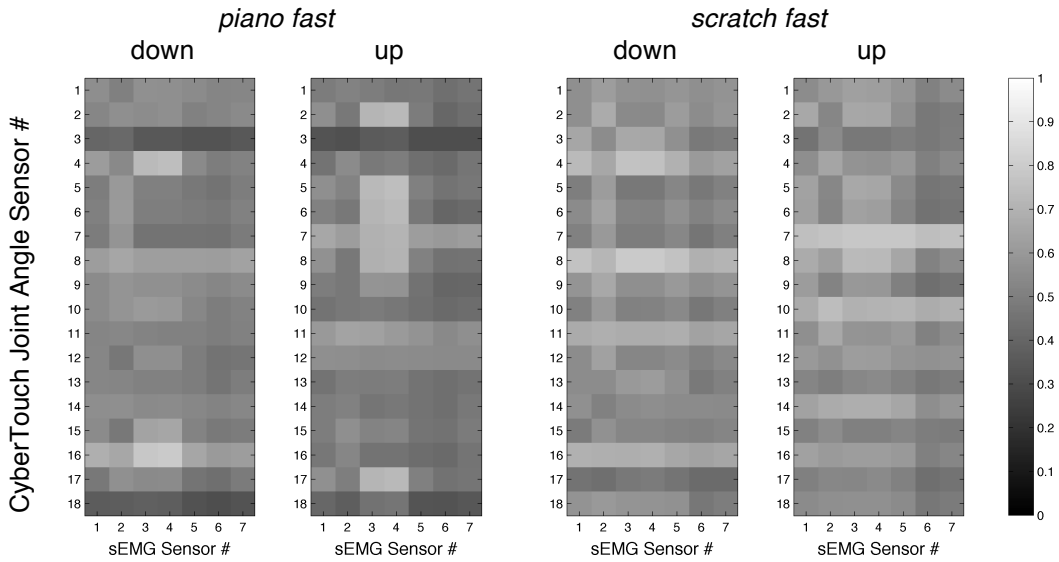

Figure 26. Correlation coefficient matrices for fast piano and scratch motion primitives for the index finger

Figure 26 shows the correlation matrices for the *piano fast* and *scratch fast* experiment.

Piano fast: The down portion of the *piano fast* motion primitive did not achieve the expected levels of correlation predicted from the biomechanical linkages. While the correlation values for the region of interest (the area including (5,5), (6,5), (7,5), (5,6), (6,6), and (7,6)) ranged between .47 and .51, which spans the border between medium and strong correlation, I would have expected the results to be stronger. An unexpected result were high correlation values for the Extensor Digiti Minimi, represented in the area including (2,5) and (2,6). This may be accounted for by the pinkie finger's extensor acting to prevent the pinkie from moving while the index finger was moving down. It is possible that there are deeply ingrained physiological and mental synergies between the fingers that do not account for the synthetic and isolated movements of the motion primitives.

Perhaps better correlations would have been seen if, instead of having the subject pause between the individual motion primitives and only performing 3 repetitions, the subject were asked to perform the motions without any pause, and to perform a larger number of repetitions so as to better familiarize the body and mind with these somewhat atypical movements. Additionally, since these motion primitives were performed at the very beginning of the experimental procedure, the subject was still adapting to the somewhat artificial task of moving single digits in isolation. It is possible that, by repeating the entire procedure multiple times, the subject might become better versed, generally, in the performance of these highly artificial motions and thereby increase the correlations for this motion primitive.

In sharp contrast, the results of the up portion of the *piano fast* motion primitive very closely matched the predictions. Moreover, the magnitudes of the correlation values were better than I would have expected for a complex physiological process. The correlation values ranged between .71 and .75, which represents a very reliable correlation between the two data streams.

Scratch fast: The results of the down portion of the *scratch fast* motion primitive were better than those for the *piano fast* down, particularly with respect to the movement of the PIJ, which would have been more dominant in this motion primitive. Overall, however, the magnitudes of the correlations, which ranged between .47 and .57 (with an average of .52). Though still considered strong by the guidelines for interpretation published by Cohen (1988), they were not as high as I had expected.

The results of the up portion of the *scratch fast* motion primitive reflected the predictions quite well. In addition to the overall strong correlation values, ranging between .62 and .66, the correlation values were evenly distributed across the Extensor Digitorum and the Extensor Indicis—the two muscles controlling the extension of the index finger from the scratch down position.

3rd Digit (middle finger)

Two motion primitives were analyzed for the middle finger: *piano fast* and *scratch fast*. Figure 27 shows the areas of interest where my hypothesis predicts elevated correlation values.

Motion capture for the *piano fast* motion primitive was primarily sampled by CyberTouch joint angle sensor number 5, although some movement would be impossible to avoid in the PIJ (middle knuckle), sampled by sensor 6. The downward movement (flexion) of the finger at the MPJ is controlled by the Flexor Digitorum Superficialis (sEMG sensors 5, 6, and 7), while the upward motion (extension) is controlled by the Extensor Digitorum (sEMG sensors 3 and 4).

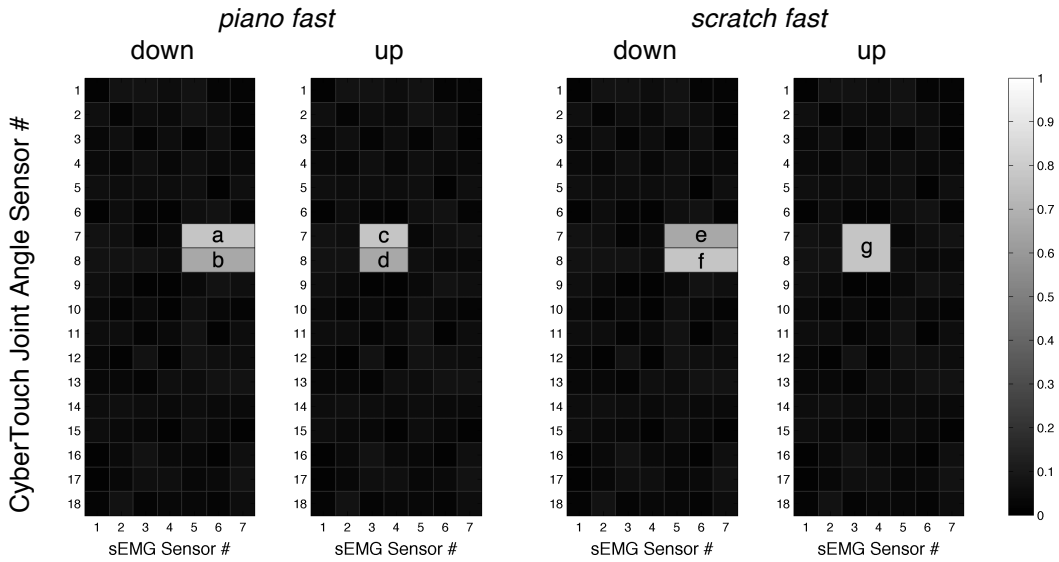

Figure 27. Predicted areas of high correlation for fast piano and scratch motion primitives for the middle finger based on biomechanical linkages

During flexion, one would expect to see higher correlations in the region labeled a in Figure 27 (the area including (5,7), (6,7), and (7,7)), and (to a lesser extent) due to inadvertent movement of the PIJ, some higher correlation values in the region labeled b (the area including (5,8), (6,8), and (7,8)). Alternatively, during extension, one would expect to see higher correlation in the region labeled c (the area including (3,7) and (4,7)). Also, as was the case for flexion, inadvertent movement of the PIJ could result in higher correlation values in the region labeled d (the area including (3,8) and (4,8)).

Hypothesis 3 predicts some degree of alternation in the aforementioned regions between the flexion and extension portions of the motion primitive, such that the lighter areas of higher correlation for flexion should be markedly darker for extension, and vice versa.

Motion capture for the *scratch fast* motion primitive was sampled by CyberTouch joint angle sensors 5 and 6. The downward movement (flexion) of the finger at the PIJ is controlled by the Flexor Digitorum Profundus and at the MPJ by the Flexor Digitorum Superficialis (sEMG sensors 5, 6, and 7), while the upward motion (extension) is controlled by the Extensor Digitorum (sEMG sensors 3 and 4).

As such, during flexion, one would expect to see higher correlation in the regions labeled e and f (the area including (5,7), (6,7), (7,7), (5,8), (6,8), and (7,8)). Due to a greater degree of movement for the PIJ than the MPJ in this motion primitive, correlation should be slightly higher in the region labeled f (the area including (5,8), (6,8), and (7,8)) than the region labeled e (the area including (5,7), (6,7), and (7,7)). Alternatively, during extension, one would expect to see higher correlation in the region labeled g (the area including (3,7), (4,7), (3,8), and (4,8)).

Hypothesis 3 predicts some degree of alternation in the aforementioned regions between the flexion and extension portions of the motion primitive, such that the lighter areas of higher correlation for flexion should be markedly darker for extension, and vice versa.

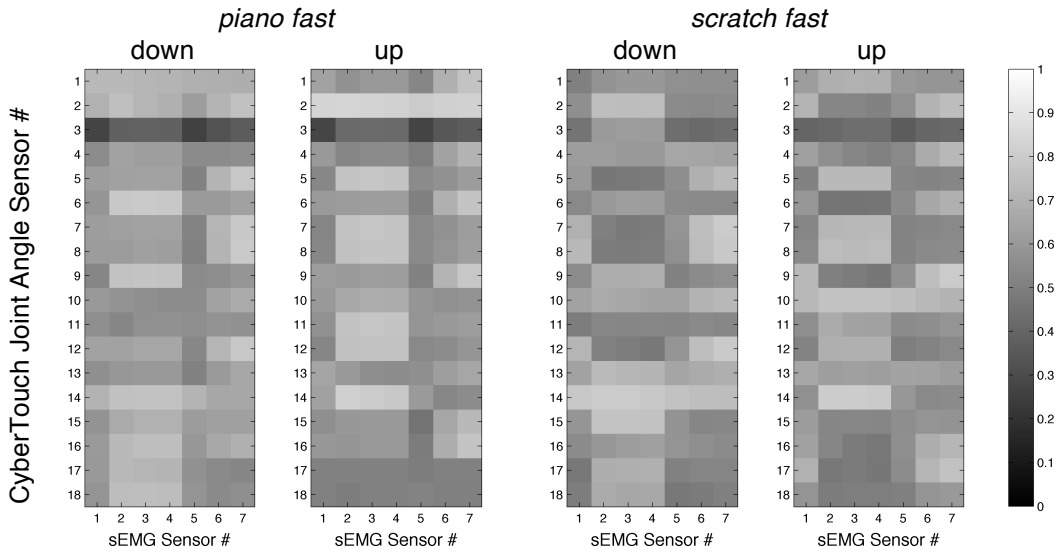

Figure 28. Correlation coefficient matrices for fast piano and scratch motion primitives for the middle finger

Figure 28 shows the correlation matrices for the *piano fast* and *scratch fast* experiment.

Piano fast: The results of the down portion of the *piano fast* motion primitive were very positive. Although, not all of the area of interest is evenly characterized by high correlation values, it is important to remember that the three sEMG sensors responsible for sampling the flexor muscles were arranged in an array and, as such, not every sensor picked up the same portion of the underlying muscle signal. The area including (5,7) and (5,8) (sEMG sensor 5 and the joint angle sensors for the middle finger) has only an average correlation value of 0.514. This is still considered a strong correlation, but at the very low end of that designation. However, sEMG sensors 6 and 7 display much larger correlation values. The average correlation value for sEMG sensor 6 and the middle finger joint angle sensors (the area including (6,7) and (6,8)) is 0.711 and the average correlation value for sEMG sensor 7 and the middle finger joint angle sensors (the

area including (7,7) and (7,8)) is .791. It would be reasonable to assume that sEMG sensor 7 is closest to the belly of the muscle responsible for flexing the middle finger. That later correlation value represents an extremely robust correlation, and one that would be considered highly dependable for the purposes of signal separation.

The results for the up portion of the *piano fast* motion primitive are equally encouraging. The area of interest for these results is the area including (3,7) and (4,8) and the average correlation value for this region is 0.771. Again, this magnitude of correlation is very robust and is characteristic of highly dependable correlation between the two data streams.

Scratch fast: The results for the down portion of the *scratch fast* motion primitive are quite similar to the down portion of the *piano fast* motion primitive, in that the relevant area of the underlying muscle appears to be located on the far end of the three sensor array. The average correlation value for sEMG sensor 5 and the middle finger joint angle sensors (the area including (5,7) and (5,8)) is 0.575, for sEMG sensor 6 and the middle finger joint angle sensors (the area including (6,7) and (6,8)) is 0.741, and the average correlation value for sEMG sensor 7 and the middle finger joint angle sensors (the area including (7,7) and (7,8)) is .790.

The results for the up portion of the *scratch fast* motion primitive also agreed with the predicted values well. The area of interest for these results is the area including (3,7), (4,7), (3,8), and (4,8) and the average correlation value for this region is 0.729. While this correlation is slightly lower than the correlation

values for the down portion of the *piano fast* motion primitive, they are, nonetheless, very high, and would form a dependable basis for the supervised machine learning techniques required to separate the blended electromyographic signals.

4th Digit (ring finger)

Two motion primitives were analyzed for the ring finger: *piano fast* and *scratch fast*. Figure 29 shows the areas of interest where my hypothesis predicts elevated correlation values.

Motion capture for the *piano fast* motion primitive was primarily sampled by CyberTouch joint angle sensor number 5, although some movement would be impossible to avoid in the PIJ (middle knuckle), sampled by sensor 6. The downward movement (flexion) of the finger at the MPJ is controlled by the Flexor Digitorum Superficialis (sEMG sensors 5, 6, and 7), while the upward motion (extension) is controlled by the Extensor Digitorum (sEMG sensors 3 and 4).

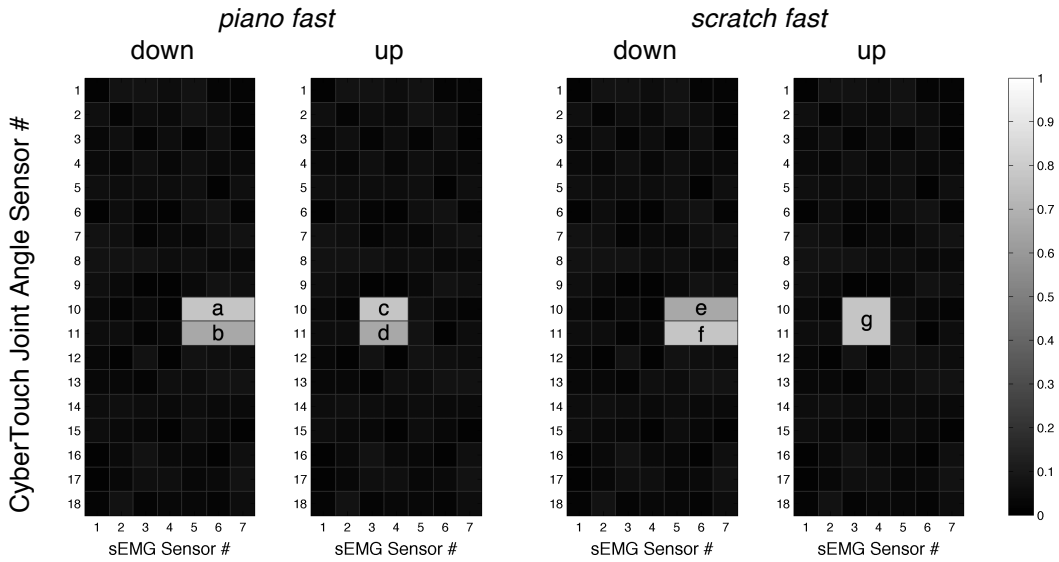

Figure 29. Predicted areas of high correlation for fast piano and scratch motion primitives for the ring finger based on biomechanical linkages

During flexion, one would expect to see higher correlations in the region labeled a (the area including (5,10), (6,10), and (7,10)), and, to a lesser extent, due to inadvertent movement of the PIJ, some higher correlation values in the region labeled b (the area including (5,11), (6,11), and (7,11)). Alternatively, during extension, one would expect to see higher correlation in the region labeled c (the area including (3,10) and (4,10)). Also, as was the case for flexion, inadvertent movement of the PIJ could result in higher correlation values in the region labeled d (the area including (3,11) and (4,11)).

Hypothesis 3 predicts some degree of alternation in the aforementioned regions between the flexion and extension portions of the motion primitive, such that the lighter areas of higher correlation for flexion should be markedly darker for extension, and vice versa.

Motion capture for the *scratch fast* motion primitive was sampled by CyberTouch joint angle sensors 5 and 6. The downward movement (flexion) of the finger at the PIJ is controlled by the Flexor Digitorum Profundus and at the MPJ by the Flexor Digitorum Superficialis (sEMG sensors 5, 6, and 7), while the upward motion (extension) is controlled by the Extensor Digitorum (sEMG sensors 3 and 4).

As such, during flexion, one would expect to see higher correlation in the regions labeled e and f (the area including (5,10), (6,10), (7,10), (5,11), (6,11), and (7,11)). Due to a greater degree of movement for the PIJ than the MPJ in this motion primitive, correlation should be slightly higher in the region labeled f (the area including (5,11), (6,11), and (7,11)) than the region labeled e (the area including (5,10), (6,10), and (7,10)). Alternatively, during extension, one would expect to see higher correlation in the region labeled g (the area including (3,10), (4,10), (3,11), and (4,11)).

Hypothesis 3 predicts some degree of alternation in the aforementioned regions between the flexions and extensions, such that the lighter areas of higher correlation for flexion should be markedly darker for extension, and vice versa.

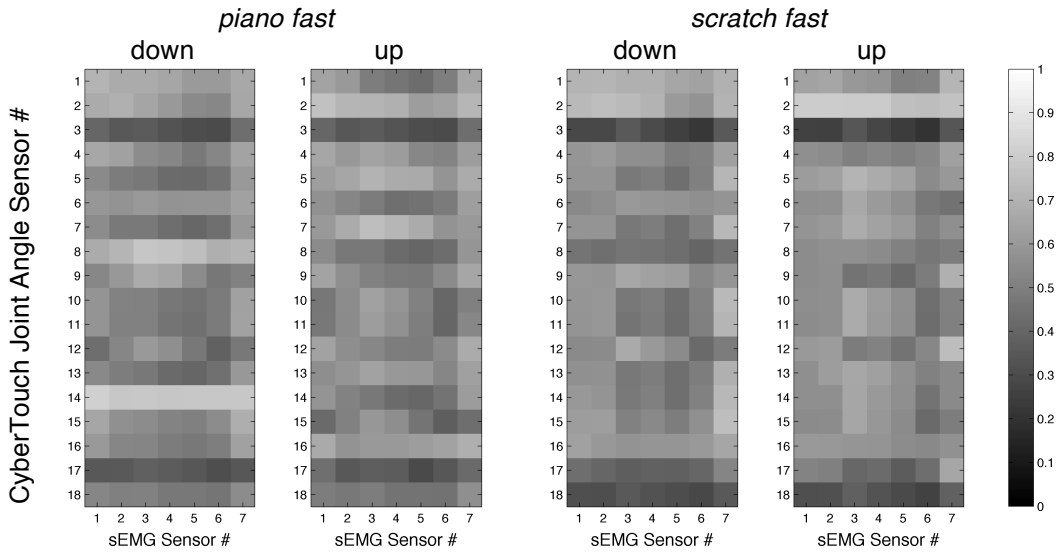

Figure 30. Correlation coefficient matrices for fast piano and scratch motion primitives for the ring finger

Figure 30 shows the correlation matrices for the *piano fast* and *scratch fast* experiment.

Piano fast: The results of the down portion of the *piano fast* motion primitive matched the predicted values well. Much like the results for the middle finger, the three sEMG sensors that constitute this array are not centered over the active muscle responsible for the flexion of the finger being examined. Rather, it appears that the portion of the Flexor Digitorum Superficialis responsible for the flexion of the MPJ of the ring finger is at the very edge of the array, and likely outside of the array, proper. The 7th sEMG sensor is still close enough to pick up a good portion of the electromyographic signal, but the rest of the array is not. The results of this portion of the experiment are as follows: the average correlation value for sEMG sensor 5 and the ring finger joint angle sensors (the area including (5,10) and (5,11)) is 0.446, for sEMG sensor 6 and the ring finger joint angle sensors (the area including (6,10) and (6,11)) is 0.482, and the average

correlation value for sEMG sensor 7 and the ring finger joint angle sensors (the area including (7,10) and (7,11)) is .633; this later result being a strong correlation.

The up portion of the *piano fast* motion primitive closely matched the predicted values. The area of interest for these results is the area including (3,10), (4,10), (3,11), and (4,11) and the average correlation value for this region is 0.603. I should note that there is a higher average correlation value for sEMG sensor 3 and the ring finger joint angle sensors (the area including (3,10) and (3,11)), which is 0.624, while the average correlation value for sEMG sensor 4 and the ring finger joint angle sensors (the area including (4,10) and (4,11)) is 0.581.

Scratch fast: The results for the down portion of the *scratch fast* motion primitive, like the down portion of the *piano fast* motion primitive reflect the predicted outcomes quite well. Again, like the down portion of the *piano fast* motion primitive, the active portion of the relevant muscle is likely at the edge of the three sEMG sensor array, though not to the same extent. This muscle, the Flexor Digitorum Profundus, responsible for flexing the PIJ, appears to be more substantially within the pick up range of sEMG sensor number 7. The results of this portion of the experiment are as follows: the average correlation value for sEMG sensor 5 and the ring finger joint angle sensors (the area including (5,10) and (5,11)) is 0.429, for sEMG sensor 6 and the ring finger joint angle sensors (the area including (6,10) and (6,11)) is 0.506, and the average correlation value

for sEMG sensor 7 and the ring finger joint angle sensors (the area including (7,10) and (7,11)) is .720; the final result being extremely robust.

The up portion of the motion primitive reflected the predicted values very well. The area of interest for these results is the area including (3,10), (4,10), (3,11), and (4,11) and the average correlation value for this region is 0.642. Even more so than the up portion of the *piano fast* motion primitive, there is a higher average correlation value for sEMG sensor 3 and the ring finger joint angle sensors (the area including (3,10) and (3,11)), which is 0.674, while the average correlation value for sEMG sensor 6 and the ring finger joint angle sensors (the area including (4,10) and (4,11)) is 0.610.

5th Digit (pinkie finger)

Two motion primitives were analyzed for the pinkie finger: *piano fast* and *scratch fast*. Figure 31 shows the areas of interest where my hypothesis predicted elevated correlation values.

Motion capture for the *piano fast* motion primitive was primarily sampled by CyberTouch joint angle sensor number 5, although some movement would be impossible to avoid in the PIJ (middle knuckle), sampled by sensor 6. The downward movement (flexion) of the finger at the MPJ is controlled by the Flexor Digitorum Superficialis (sEMG sensors 5, 6, and 7), while the upward motion (extension) is controlled by the Extensor Digitorum (sEMG sensors 3 and 4) and, to a lesser degree, the Extensor Digiti Minimi (sEMG sensor 2).

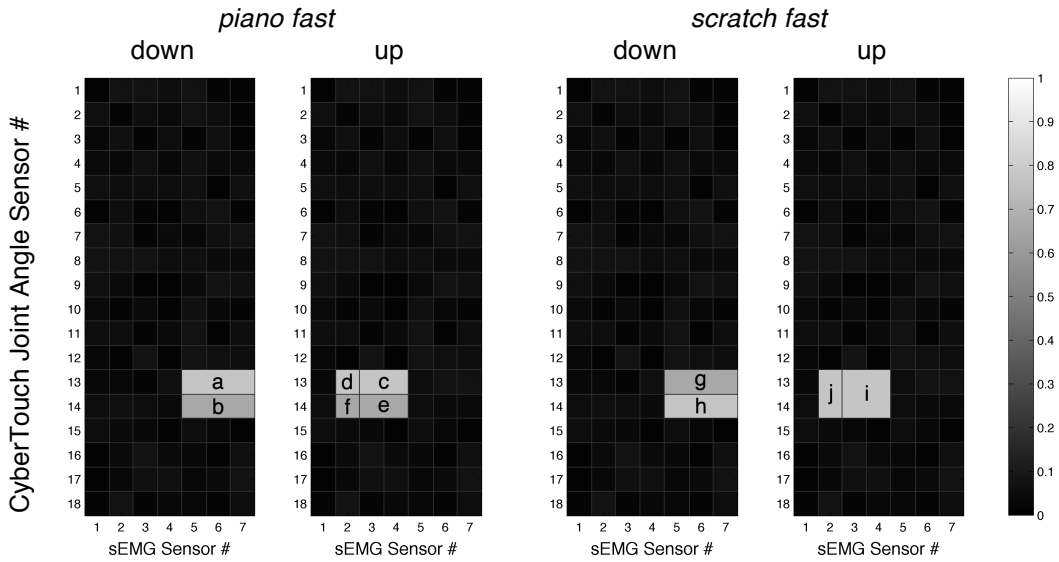

Figure 31. Predicted areas of high correlation for fast piano and scratch motion primitives for the pinkie finger based on biomechanical linkages

During flexion, one would expect to see higher correlation in the region labeled a (the area including (5,13), (6,13), and (7,13)), and (to a lesser extent) due to inadvertent movement of the PIJ, some higher correlation values in the region labeled b (the area including (5,14), (6,14), and (7,14)). Alternatively, during extension, one would expect to see higher correlation values in the region labeled c (the area including (3,13) and (4,13)), and, due to slight contribution form the Extensor Digiti Minimi, an increase in the correlation values in the region labeled d (cell (2,13)). Also, as was the case for flexion, inadvertent movement of the PIJ could result in higher correlation values in the region labeled e (the area including (3,14) and (4,14)) as well as in the region labeled f (cell (2,14)).

Hypothesis 3 predicts some degree of alternation in the aforementioned regions between the flexion and extension portions of the motion primitive, such

that the lighter areas of higher correlation for flexion should be markedly darker for extension, and vice versa.

Motion capture for the *scratch fast* motion primitive was sampled by CyberTouch joint angle sensors 5 and 6. The downward movement (flexion) of the finger at the PIJ is controlled by the Flexor Digitorum Profundus and at the MPJ by the Flexor Digitorum Superficialis (sEMG sensors 5, 6, and 7), while the upward motion (extension) is controlled by the Extensor Digitorum (sEMG sensors 3 and 4) and, to a greater degree than for the *piano fast* motion primitive, the Extensor Digiti Minimi (sEMG sensor 2).

As such, during flexion, one would expect to see increased correlation in the regions labeled g and h (the area including (5,13), (6,13), (7,13), (5,14), (6,14), and (7,14)). Due to a greater degree of movement for the PIJ than the MPJ in this motion primitive, correlation values should be slightly higher in the region labeled h (the area including (5,14), (6,14), and (7,14)) than in the region labeled g (the area including (5,13), (6,13), and (7,13)).

Alternatively, during extension, one would expect to see increased correlation in the region labeled i (the area including (3,13), (4,13), (3,14), and (4,14)) with a roughly similar correlation value for the region labeled j (the area including (2,13) and (2,14)) due to the significant contribution from the Extensor Digiti Minimi.

Hypothesis 3 predicts some degree of alternation in the aforementioned regions between the flexions and extensions, such that the lighter areas of higher correlation for flexion should be markedly darker for extension, and vice versa.

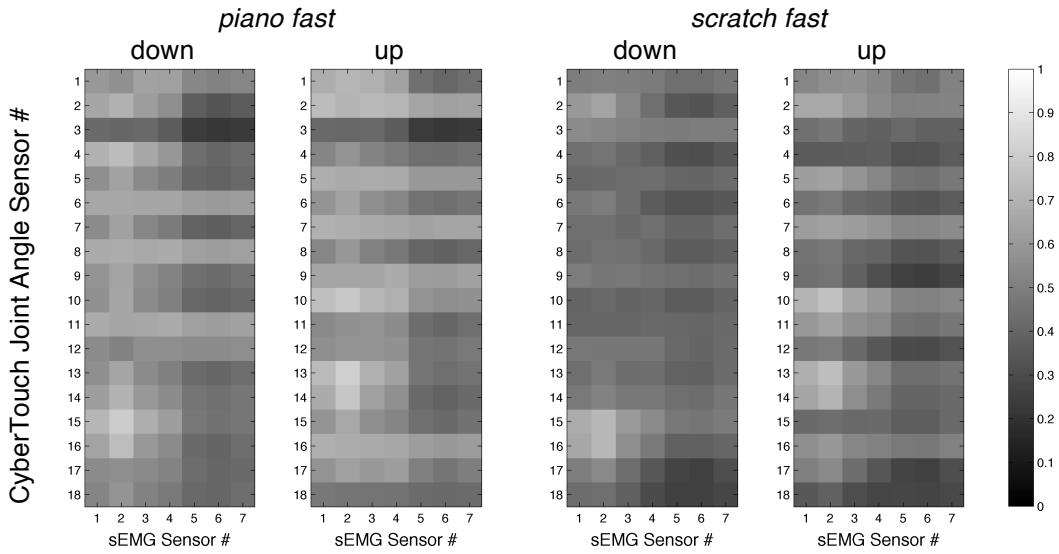

Figure 32. Correlation coefficient matrices for fast piano and scratch motion primitives for the pinkie finger

Figure 32 shows correlation matrices for the *piano fast* and *scratch fast* experiment.

Piano fast: The results for the down portion of the *piano fast* motion primitive did not reflect the predictions made based on the biomechanical linkages. As was becoming clear with the middle finger and the ring finger, the active portion of the Flexor Digitorum Superficialis was moving gradually outside of the pick up area of the sEMG sensor array. For the pinkie finger, it appears that the electromyographic signal was no longer in range of any of the three sEMG sensors and. As such, the average correlation value for the region of interest (the area including (5,13), (6,13), (7,13), (5,14), (6,14), and (7,14)) was 0.440—a figure slightly below the threshold for a strong correlation. I believe that if an additional sensor were placed at the end of this array, its correlation values would have been higher.

The results for the up portion of the motion primitive, on the other hand, were encouraging. The average correlation values between the Extensor Digitorum and the knuckles of the pinkie finger (the area including (3,13), (3,14), (4,13), and (4,14)) were 0.629. The average correlation value between the Extensor Digiti Minimi—the dedicated extensor for the pinkie finger—and the joint angle sensors for the pinkie finger (the area including (2,13) and (2,14)) was a very robust 0.792. Additionally, the correlation value for the Extensor Digiti Minimi and the MPJ—the primary joint active in this motion primitive (cell (2,13)) was 0.809.

Scratch fast: The results for the down portion of the motion primitive, like the *piano fast* motion primitive, did not reflect the predictions made based on the biomechanical linkages. Just as the Flexor Digitorum Superficialis, the active area of the Flexor Digitorum Profundus appears to have moved completely outside of the pick up area of the sEMG sensor array. The average correlation value for the region of interest (the area including (5,13), (6,13), (7,13), (5,14), (6,14), and (7,14)) was 0.421—a figure below the threshold for a strong correlation. Again, I believe that if an additional sensor were placed at the end of this array, its correlation values would have been higher.

The results for the up portion of the motion primitive did reflect the predictions quite well. The average correlation value between the Extensor Digitorum and the knuckles of the pinkie finger (the area including (3,13), (4,13), (3,14), and (4,14)) was 0.541. For this motion primitive, the Extensor Digiti Minimi was more prominent than in *piano fast*. This is well reflected in the

average correlation values between the Extensor Digiti Minimi and the joint angle sensors for the pinkie finger (the area including (2,13) and (2,14)), which was a very robust 0.725.

Summary

In general, the matrices in Figure 26, Figure 28, Figure 30, and Figure 32 show high correlations where they are predicted based on the biomechanical connections described earlier in this chapter, and show lower correlations in the other areas. In those cases where correlations were less strong, modifications of the experimental procedure as well as augmentation of the number of sensors utilized in the arrays were proposed as a means to strengthening the correlations in a future experiment. However, overall, the results do suggest that statistical methods (such as supervised learning) could be used to separate the blending of muscle activation signals seen in the sEMG signals. Further research is clearly warranted.

CHAPTER 6

DISCUSSION

Faced with the constraints of having to develop mass produced products, designers have often encountered the insurmountable problem of trying to design a single product to satisfy the diverse (and often contradictory) needs of large human populations. The approach of developing broad archetypes from studies of human populations (and then using those archetypes to design just a few solutions to serve the entire and diverse population) serves the needs of manufacturers better than the needs of users. Many of these products are ultimately judged to be inadequate across a large portion of that population. Some of these products are even responsible for harm or injury to some users.

One example of this is the QWERTY keyboard (developed by Christopher Sholes in 1878) whose design has survived virtually unchanged for well over a century, and whose use is ubiquitous in computer keyboards today. This despite nearly a century of experience and research that show the adverse long-term health risks associated with its use. Interestingly, not all users are adversely affected, leading me to hypothesize that the cause was a mismatch between the repetitive hand motions involved in using the keyboard, and the natural hand motions of some susceptible individuals. Thus, my research efforts began with the aim of developing an alternative method for entering text into computers—one that allowed for the use of *individualized* hand gesture alphabets tailored to

the unique physical attributes of each user—the goal being to avoid any adverse health consequences.

However, upon launching into the study it soon became clear that, although the long-term health risks across populations were well documented there was no method for reliably predicting the long-term health risks to individual users. The testing methods themselves were based on archetypal models of human physiology, and they had produced inconclusive and contradictory results for alternative data entry designs that had already been tested. Apparently, if an alternative was developed, there was no reliable way to use short-term studies to evaluate whether that alternative would be superior to existing keyboard input methods, over the long term for each individual user. This fact shifted my focus from the development of an alternative design for text input to the development of a method for assessing the health impact of an alternative design on each individual user during the course of real use.

Use of Electromyography for Monitoring Muscle Health

Needle-based EMG had long been established as a reliable method for the measurement of the neuromuscular impact of product usage. In fact, it has even been referred to as the *gold standard*. However, needle-based EMG is impractical for use in studies of the human forearm, because the needles must be inserted through *layers* of lower arm musculature, to reach the deeper muscles. The alternative *surface* EMG has been used to study neuromuscular impact on large muscle groups, such as the upper leg. However, it has been ineffective when used

on the lower arm, because the electrical signals from the various muscles become *mixed* as they propagate toward the surface of the skin.

Thus, the challenge was to explore the possibility of developing a method for separating the mixed signals produced by non-invasive surface EMG, to allow evaluation of the state of the individual muscles in the forearm. The results produced by the methods outlined in this thesis indicate that it is possible to use non-invasive surface EMG signals to monitor the activity of individual muscle groups within the human forearm, thus allowing the analysis of the health effects of device usage on the forearm of each individual user.

Further Research

Refinement of Experiment Design

The results of this research support the hypothesis that machine learning could be used to separate the mixed signals collected from surface EMG sensors on a human forearm into their constituent muscle signals. However, additional work will be needed to further refine the method for doing so. Some very useful lessons were learned during the performance of these experiments that could be used to improve the measured correlations that were observed between the activation of the muscle groups and the individual finger motions.

First of all, the hand movements that were used in these experiments to isolate the usage of the individual muscle groups in the forearm were somewhat different from those used by the subjects in their normal day-to-day activities, where muscle groups in the forearm are typically used together. When first

attempting these hand movements, subjects found them to be somewhat awkward, and the isolation was less than ideal. Part of the problem was that only 3 temporally spaced repetitions of each hand motion were used during the experiment, and this did not allow much time for the subject to become accustomed to these novel hand motions. It is possible that better results could be achieved if the subjects were asked to perform the hand motions smoothly, without an artificial pause, and to perform a larger number of repetitions, so as to become better familiarized with these somewhat atypical hand movements. This hypothesis is supported by the fact that some of the hand motions that were performed at the very beginning of the experimental procedure yielded lower correlations than those same hand motions performed later.

Secondly, it is possible that better correlation values would be seen if some method were developed to accelerate the learning of the novel hand motions. For example, a *brace* could be employed for the arms and fingers, to block the motion of fingers that are supposed to remain stationary – thus providing the subject with some proprioceptive feedback indicating when the proper hand motions were being executed. With repetitions of the hand motion against the brace, the subject would learn which muscles need to be activated, and which should remain relaxed.

Thirdly, given the number of muscle groups in the forearm, the use of additional surface EMG sensors would provide additional signals that would facilitate the separation of the signals of the individual muscle groups. In

particular, additional sensors over the *Flexor Digitorum Superficialis* and the *Flexor Digitorum Profundus* would be helpful.

Additional Analysis

The *Flexor Digitorum Superficialis* and the *Flexor Digitorum Profundus* were each sampled by an array of sensors. It is possible that an analysis of the correlation between the movement of the individual fingers and some *function of the array* of signals (instead of the correlation between the finger movement and each *individual* signal) would yield higher correlation values.

Machine Learning

The correlation values produced by these experiments between the individual finger motions and the surface EMG signals show that a machine learning algorithm could be trained to largely separate the mixed surface EMG signals from the surface of the forearm. In order to validate these separated signals, a simultaneous experiment could be conducted using needle-based EMG, in addition to the surface EMG used in these experiments. The results from the invasive needle-based EMG sensors could then be used as a *ground truth*, against which the separated signals from the machine learning algorithm could be compared.

Due to the high degree of biomechanical linkage between the extrinsic hand muscles located in the forearm, and the individual fingers of the hand, it could then be possible to train a machine learning algorithm to track the

movement of the fingers based solely on the signals from the surface EMG sensors. However, it is important to emphasize that such a system would need to be trained for each individual user, one at a time.

Developing an Alternative Text Entry Method

Once a reliable mechanism has been developed for non-invasively assessing the health of the forearm muscle groups in real time, it would be possible to define a set of customized set of hand postures for each individual. That set of hand postures would be based on the postures that the individual generates most often, and could be used for alphanumeric data entry.

This would allow for testing of the hypothesis that, if a system of data entry is based solely on the postures that the individual generates with the greatest frequency, then the use of this system would result in lower fatigue, and a lower incidence of pathologies, as compared to one-size-fits-all hand postures, such as those used for ASL fingerspelling. Because surface EMG is non-invasive, it could then be used to conduct continuous assessment of muscle health for each individual, over a long period of use.

REFERENCES

Amell, T. K., & Kumar, S. (2000). Cumulative trauma disorders and keyboarding work. *International Journal of Industrial Ergonomics, 25*(1), 69-78. doi: 10.1016/s0169-8141(98)00099-7

Bao, S., Howard, N., Spielholz, P., & Silverstein, B. (2006). Quantifying repetitive hand activity for epidemiological research on musculoskeletal disorders–Part II: comparison of different methods of measuring force level and repetitiveness. *Ergonomics, 49*(4), 381-392. doi: 10.1080/00140130600555938

Bao, S., Silverstein, B., & Cohen, M. (2001). An electromyography study in three high risk poultry processing jobs. *International Journal of Industrial Ergonomics, 27*(6), 375-385. doi: 10.1016/s0169-8141(01)00004-x

Basmajian, J. V., & De Luca, C. J. (1985). *Muscles alive: their functions revealed by electromyography* (5th ed.). Baltimore: Williams & Wilkins.

Bergamasco, R., Girola, C., & Colombini, D. (1998). Guidelines for designing jobs featuring repetitive tasks. *Ergonomics, 41*(9), 1364-1383. doi: 10.1080/001401398186379

Bourke, P. (1999). Interpolation methods, from http://paulbourke.net/miscellaneous/interpolation/

Brown, J. N. A., Albert, W. J., & Croll, J. (2007). A new input device: comparison to three commercially available mouses. *Ergonomics, 50*(2), 208-227. doi: 10.1080/00140130601002609

Brown, S., Lamming, R., Bessant, J., & Jones, P. (2004). *Strategic operations management* (2nd ed.). Boston, MA: Elsevier.

Burgess-Limerick, R., Shemmell, J., Scadden, R., & Plooy, A. (1999). Wrist posture during computer pointing device use. *Clinical Biomechanics, 14*(4), 280-286. doi: 10.1016/s0268-0033(98)90093-6

Clancy, E. A., Morin, E. L., & Merletti, R. (2002). Sampling, noise-reduction and amplitude estimation issues in surface electromyography. *Journal of Electromyography and Kinesiology, 12*(1), 1-16. doi: 10.1016/S1050-6411(01)00033-5

Cohen, J. (1988). *Statistical power analysis for the behavioral sciences* (2nd ed.). Hillsdale, N.J.: L. Erlbaum Associates.

Cook, T., Rosecrance, J., Zimmermann, C., Gerleman, D., & Ludewig, P. (1998). Electromyographic Analysis of a Repetitive Hand Gripping Task. *International Journal of Occupational Safety and Ergonomics, 4*(2), 185-200.

Da Silveira, G., Borenstein, D., & Fogliatto, F. S. (2001). Mass customization: Literature review and research directions. *International Journal of Production Economics, 72*(1), 1-13. doi: 10.1016/S0925-5273(00)00079-7

Davis, S. M. (1987). *Future perfect*. Reading, Mass.: Addison-Wesley.

Dipietro, L., Sabatini, A., & Dario, P. (2008). A Survey of Glove-Based Systems and Their Applications. *IEEE Transactions on Systems, Man, and Cybernetics, Part C (Applications and Reviews), 38*(4), 461-482. doi: 10.1109/TSMCC.2008.923862

Dirjish, M. (2008). From the typewriter to the PC and beyond. *Electronic Design, 56*(12), 69-72.

Duguay, C. R., Landry, S., & Pasin, F. (1997). From mass production to flexible/agile production. *International Journal of Operations & Production Management, 17*(12), 1183-1195. doi: 10.1108/01443579710182936

Dvorak, A. (1943). There is a better typewriter keyboard. *National Business Education Quarterly, 11*(2), 51-58.

Erdil, M., & Dickerson, O. B. (Eds.). (1997). *Cumulative trauma disorders: prevention, evaluation, and treatment*: Van Nostrand Reinhold.

Fagarasanu, M., & Kumar, S. (2003). Carpal tunnel syndrome due to keyboarding and mouse tasks: a review. *International Journal of Industrial Ergonomics, 31*(2), 119-136.

Feuerstein, M., Armstrong, T., Hickey, P., & Lincoln, A. (1997). Computer keyboard force and upper extremity symptoms. *Journal of Occupational and Environmental Medicine, 39*(12), 1144-1153. doi: 10.1097/00043764-199712000-00008

Fogleman, M., & Brogmus, G. (1995). Computer mouse use and cumulative trauma disorders of the upper extremities. *Ergonomics, 38*(12), 2465-2475.

Fralix, M. T. (2001). From mass production to mass customization. *Journal of Textile and Apparel, Technology and Management, 1*(2), 1-7.

Gerard, M. J., Jones, S. K., Smith, L. A., Thomas, R. E., & Wang, T. (1994). An ergonomic evaluation of the Kinesis ergonomic computer keyboard. *Ergonomics, 37*(10), 1661-1668.

Hedge, A., & Powers, J. R. (1995). Wrist postures while keyboarding: effects of a negative slope keyboard system and full motion forearm supports. *Ergonomics, 38*(3), 508-517.

Hermens, H., Hägg, G., & Freriks, B. (1997). *SENIAM 2: European applications on surface electromyography.* Paper presented at the The Second General SENIAM Workshop, Stockholm, Sweden.

Hirsch, B. E., Thoben, K. D., & Hoheisel, J. (1998). Requirements upon human competencies in globally distributed manufacturing. *Computers in Industry, 36*(1-2), 49-54. doi: 10.1016/s0166-3615(97)00097-3

Iridiastadi, H., & Nussbaum, M. A. (2006). Muscle fatigue and endurance during repetitive intermittent static efforts: development of prediction models. *Ergonomics, 49*(4), 344-360. doi: 10.1080/00140130500475666

Kamen, G., & Caldwell, G. E. (1996). Physiology and interpretation of the electromyogram. *Journal of Clinical Neurophysiology, 13*(5), 366-384.

Kanchanasevee, P., Biswas, G., Kawamura, K., & Tamura, S. (1997). *Contract-net-based scheduling for holonic manufacturing systems.* Paper presented at the Architectures, Networks, and Intelligent Systems for Manufacturing Integration, Pittsburgh, PA, USA.

Keir, P. J., & Wells, R. P. (2002). The Effect of Typing Posture on Wrist Extensor Muscle Loading. *Human Factors, 44*(3), 392-403.

Keyserling, W. M., Stetson, D. S., Silverstein, B. A., & Brouwer, M. L. (1993). A checklist for evaluating ergonomic risk factors associated with upper extremity cumulative trauma disorders. *Ergonomics, 36*(7), 807-831. doi: 10.1080/00140139308967945

King, W. R. (1998). IT-Enhanced Productivity and Profitability. *Information Systems Management, 15*(3), 1-3. doi: 10.1201/1078/43185.15.3.19980601/31138.11

Kramer, J. P., Lindener, P., & George, W. R. (1991). 5047952. U. S. P. Office.

Mäkipää, M., & Mattila, J. (2004). Mass Customization and Beyond in Software Engineering–Developing a Framework for Mass Customized Adaptive Software. *Mäkipää, M. and Ruohonen, M.(edt.)(2004). The First Finnish Mass Customization and Personalization (MCP) Forum–Facing International Research. E-Business Research Center, Research Reports, 12*.

Marklin, R. W., & Simoneau, G. G. (2001). Effect of Setup Configurations of Split Computer Keyboards on Wrist Angle. *Physical Therapy, 81*(4), 1038-1048.

Melhorn, J. (1994). Occupational injuries: the need for preventive strategies. *Kansas medicine: the journal of the Kansas Medical Society, 95*(11), 248-251.

Morelli, D. L., Johnson, P. W., Reddell, C. R., & Lau, P. (1995). *User Preferences between Keyboards While Performing "Real" Work: A Comparison of "Alternative" and Standard Keyboards.* Paper presented at the Human Factors and Ergonomics Society 39th Annual Meeting.

Muggleton, J. M., & Allen, R. (1999). Hand and arm injuries associated with repetitive manual work in industry: a review of disorders. *Ergonomics, 42*(5), 714.

Nainzadeh, N., Malantic-Lin, A., Alvarez, M., & Loeser, A. C. (1999). Repetitive Strain Injury (Cumulative Trauma Disorder). *The Mount Sinai Journal of Medicine, 66*(3).

Norman, D. A., & Fisher, D. (1982). Why Alphabetic Keyboards Are Not Easy to Use: Keyboard Layout Doesn't Much Matter. *Human Factors: The Journal of the Human Factors and Ergonomics Society, 24*(5), 509-519. doi: 10.1177/001872088202400502

Noyes, J. (1983). The QWERTY keyboard: a review. *International Journal of Man-Machine Studies, 18*(3), 265-281. doi: 10.1016/s0020-7373(83)80010-8

O'Grady, P. (1999). *The Age of Modularity*. Iowa City, Iowa: Adams & Steele.

Ostlund, N., Yu, J., Roeleveld, K., & Karlsson, J. S. (2004). Adaptive spatial filtering of multichannel surface electromyogram signals. *Medical and Biological Engineering and Computing, 42*(6), 825-831. doi: 10.1007/BF02345217

Pascarelli, E., & Kella, J. (1993). Soft-tissue injuries related to use of the computer keyboard. *Journal of Occupational Medicine, 35*(5), 522-532.

Pine, B. J., & Davis, S. (1993). *Mass Customization: The New Frontier in Business Competition*. Boston: Harvard Business School Press.

Ritchie, J., & Black, I. (1999, 1999). *Product design and manufacturing methods-learning the historical lesson.* Paper presented at the Management of Engineering and Technology, 1999. Technology and Innovation Management. PICMET '99. Portland International Conference on, Portland, OR.

Rittel, H. W. J., & Webber, M. M. (1973). Dilemmas in a General Theory of Planning. *Policy Sciences, 4*(2), 155-169.

Sabel, C., & Zeitlin, J. (1985). Historical Alternatives to Mass Production: Politics, Markets and Technology in Nineteenth-Century Industrialization. *Past and Present*(108), 133-176.

Schwartz, M. S., & Andrasik, F. (2005). *Biofeedback: A Practitioner's Guide*: Guilford Press.

Serina, E. R., Tal, R., & Rempel, D. (1999). Wrist and forearm postures and motions during typing. *Ergonomics, 42*(7), 938-951. doi: 10.1080/001401399185225

Simon, H. A. (1996). *The Sciences of the Artificial* (3rd ed.). Cambridge, MA: MIT Press.

Spielholz, P., Silverstein, B., Morgan, M., Checkoway, H., & Kaufman, J. (2001). Comparison of self-report, video observation and direct measurement methods for upper extremity musculoskeletal disorder physical risk factors. *Ergonomics, 44*(6), 588-613. doi: 10.1080/00140130118050

Sturman, D. J., & Zeltzer, D. (1994). A survey of glove-based input. *IEEE Computer Graphics and Applications, 14*(1), 30-39. doi: 10.1109/38.250916

Swanson, N. G., Galinsky, T. L., Cole, L. L., Pan, C. S., & Sauter, S. L. (1997). The impact of keyboard design on comfort and productivity in a text-entry task. *Applied Ergonomics, 28*(1), 9-16. doi: 10.1016/S0003-6870(96)00052-X

Szabo, R. M. (1998). Carpal tunnel syndrome as a repetitive motion disorder. *Clinical orthopaedics and related research, 351*, 78.

Szeto, G. P. Y., & Ng, J. K. F. (2000). A Comparison of Wrist Posture and Forearm Muscle Activities While Using an Alternative Keyboard and a Standard Keyboard. *Journal of Occupational Rehabilitation, 10*(3), 189-197. doi: 10.1023/a:1026662302131

Toffler, A. (1980). *The Third Wave* (1st ed.). New York: Morrow.

US Bureau of Labor Statistics. (1996). Survey of occupational injuries and illnesses, 1994. *Summary 96-11*. Washington, DC: US Department of Labor.

Xu, Z., Xiao, S., & Chi, Z. (2001). ART2 Neural Network for Surface EMG Decomposition. *Neural Computing & Applications, 10*(1), 29-38. doi: 10.1007/s005210170015

APPENDIX A

APPARATUS

This section describes all of the equipment, built or acquired, that was necessary for running the experiments required to test the hypothesis articulated earlier in this paper. It will also include settings, parameters, and practices that were needed to create a single, integrated system manageable from a single control point.

Figure 33 shows a System Diagram that illustrates this consolidated apparatus as a whole. Each component will be described below. The System Diagram is provided in order to contextualize each component within the overall consolidated system.

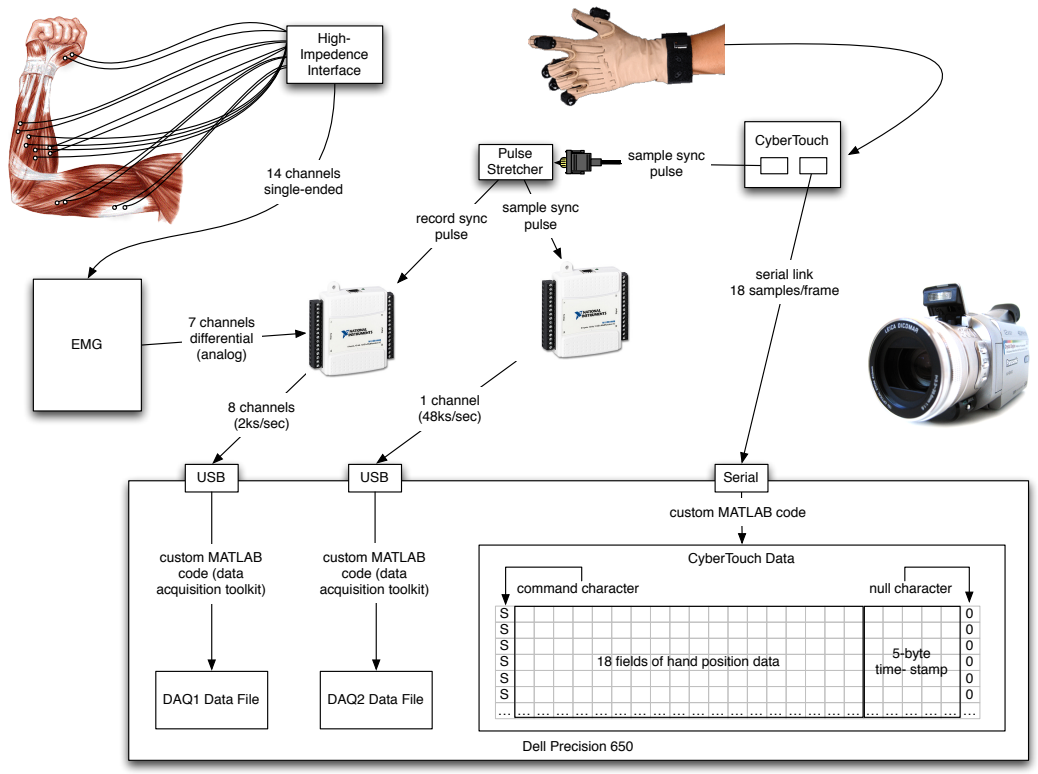

Figure 33. System Diagram

Physiological Data Capture

Hand Posture (CyberTouch)

In order to capture an accurate representation of hand posture an 18 sensor CyberTouch instrumented glove from Immersion Corporation was put onto the subject's right hand. The specifications of the glove are as follows:

- Sensor Resolution: <1°
- Sensor Repeatability: 3° (average standard deviation between wearings)
- Sensor Linearity: maximum 0.6% nonlinearity over full joint range
- Sensor Data Rate: 90 records/sec (typical)
- Interface: RS-232 (115.2 kbaud)

Figure 34. CyberTouch Instrumented Glove

Muscle Electrophysiology (sEMG)

Seven channels of electrophysiological muscle data were collected via surface skin sensors (sEMG). Signals were collected using seven pairs of model F-E14D silver/silver chloride (Ag/AgCl) pre-gelled disposable sensors manufactured by Grass Technologies. All sensors were placed in a bipolar arrangement on the right arm of each subject employing a center-to-center spacing of 20mm. Grass Technologies F-SL60 Snap Leads were affixed to each sensor and connected to a Grass Technologies High Impedance Input Module.

Figure 35. Grass Technologies F-E14D Ag/AgCl pre-gelled disposable sensor and Grass Technologies F-SL60 Snap Lead

Electrophysiological muscle data was captured with a Grass Technologies Model 8-16 C Electroencephalograph/Electromyograph bio-physiological data capture system. Seven of the sixteen available amplifiers were used. Each amplifier received as input a pair of differential signals. A single signal was derived from the differential inputs. Output amplification was calibrated to produce signals within a range of ±2.4 Volts.

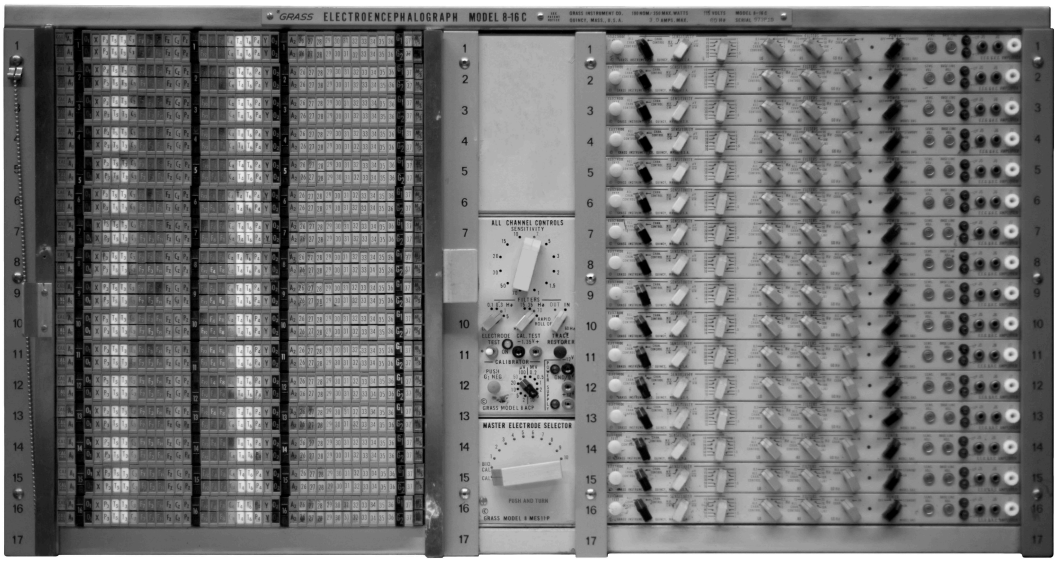

Figure 36. Grass Technologies Model 8-16 C Electroencephalograph/ Electromyograph

Digitization

Figure 37. National Instruments NI USB-6009 Multifunction DAQ

Output from the seven EMG amplifiers was digitized with a National Instruments NI USB-6009 Multifunction DAQ (DAQ2). Signals from the

amplifiers were fed to the DAQs via custom made cables with a 3.5mm jack that plugged into the output of each amplifier channel and a pair of bare wires (one signal wire and a return/ground wire), which were attached to screw-terminals on the DAQs analog input block.

The Pulse Stretcher

Figure 38. Custom designed Pulse Stretcher Unit

The frame sync pulse from the custom-made pulse stretcher was sent to the eighth channel on DAQ2. All digitization on DAQ2 was performed at 2,000

samples per second (2kHz). The record sync pulse from the pulse stretcher was sent to DAQ1, which digitized the analog signal at a rate of 48,000 samples per second (48kHz).

Control and Consolidation

The CyberTouch interface box was connected to the serial port of a Dell Precision 650 computer, equipped with dual Xeon 3.2GHz processors and with 1.5 Gb of RAM running Microsoft Windows XP Service Pack 2. The CyberTouch interface box and the Windows PC were set to their maximum serial transmission rate of 115.2 Kbps.

The two National Instruments DAQs (DAQ1 and DAQ2) were connected via USB to the Windows PC to sample the seven EMG data streams and the CyberTouch sync pulse, which was used to synchronize the CyberTouch data stream to the single master clock.

The CyberTouch was controlled and hand posture data were collected via custom software written in MATLAB v.7. The two National Instruments DAQs were controlled from, and their data were collected by custom application software written in MATLAB with extensive use of MATLAB's Data Acquisition Toolkit.

The custom MATLAB application provided a single point of control for the data collection process including: initialization of the CyberTouch, the two DAQs, the receiving ports on the computer as well as initiation of data stream capture. A second point of control managed all of the "housekeeping" processes

required for error-free completion of data captures and properly formatted data storage in MATLAB.

To guarantee synchronization between the CyberTouch data stream, the EMG data stream, and the specific movements that were requested of the subject, a video camera with a capture rate of 60 frames per second (with timecode) collected audio and video of the experimental procedure.

APPENDIX B

SUBJECT BRIEFING

The following is the text of the handout that was given to subjects when the data collection "appointment" was made.

Brief Background:

The purpose of this experiment is to determine if accurate diagnosis of the lower arm's muscles can be achieved via surface electromyography (sEMG) if the addition of information about the hand's position, velocity, and acceleration is included in the analysis.

Some requests:

Please set aside 90 minutes for the complete set of experiments.

- Please wear a loose fitting short-sleeved shirt
- During the test, it will be necessary to remove any rings, watches, bracelets, or other jewelry from your hands and arms. We will provide a bin for storage; however, it might be easier to not wear such items to the test session.
- Please refrain from applying any lotions, sunscreen, creams, or oils to your arms or hands (the areas where sEMG sensors will be attached) for a period of no less than 24 hours prior to the time of testing.

Purpose of Experiment:

The purpose of this experiment is to determine if the use of hand posture data collected from a CyberTouch instrumented glove can be used as ground truth for the decomposition of surface electromyographic data from the lower arm.

The length of the entire experiment will be approximately 90 minutes. I will begin with an explanation of what we will be doing, step by step, and you are free to ask questions at any time. Keep in mind that you are also free to quit the experiment at any time and for whatever reason.

I will begin by asking you some demographic questions. Please be assured that any personal data that is collected is for statistical analysis purposes only. Your name will be decoupled from the demographic data as well as all data that is collected so that your privacy is protected.

Attaching the Recording Apparatus:

The first piece of apparatus placed on you will be the surface electromyographic sensors. Before the sensors can be placed onto your skin, I will need to remove oil, dead skin and other debris that might interfere with the EMG's ability to make accurate readings. Removal of surface debris will be done with a mildly abrasive cleanser-infused pad.

Once your skin has had a chance to dry I will place seven pairs of electrodes onto your arm. These sensors are disposable and you will be the only person to have used them. They are attached with a mild adhesive, which should be painless to remove once the experiment has completed.

After the sensors are secured to your arm and they have had a chance to adhere, I will attach wire leads to the electrodes. These leads will be connected to the EMG. This machine is designed specifically for this type of experiment and there is no risk of electrical shock.

I will then place the CyberTouch glove onto your hand so that we can record the positions of your hand throughout the experiment.

Finally, I will place a wrist and thumb brace, commonly used for people with carpal-tunnel syndrome, onto your arm in order to minimize any movement of your wrist, forearm, and thumb.

The Experiment:

The first phase of the experiment will last 10 minutes. The purpose of this phase is to calibrate the system. I will hold your hand and fingers so that they are rested and relaxed. One finger at a time, I will ask you to slowly move each digit according to my instructions. During this time, I will be collecting data with the CyberTouch glove and the sEMG.

Once the 10-minute calibration period is over, I will guide you through a series of quasi-free movements. The purpose of my guidance will be to maximize movement of all your fingers, to increase the distribution of movements across finger combinations, and to minimize movement of your wrist and forearm.

At the conclusion of the second data collection phase, I will remove the sensors from your hand and arm and give you a chance to get up and stretch. You

may use the restroom and get something to drink. Once you are ready to continue, I will reapply the sensors and we will begin the final phase of the experiment.

The third data collection phase of the experiment will be identical to the second and, once again, I will guide your motions as necessary.

I will then help you remove the measurement devices.

Finally, I will ask you some questions regarding your experience and give you an opportunity to comment on the experiment itself.

Before we begin, I'd like to thank you for participating in this process. Your involvement is invaluable

APPENDIX C

IRB APPROVAL

ARIZONA STATE UNIVERSITY
Research Compliance Office
Office for Research & Sponsored Projects Administration
P.O. Box 873503
Tempe, AZ 85287-3503

Phone
(480) 965-6788
Facsimile
(480) 965-7772

To:	Jacques Giard AED 162
From:	Mark Roosa, Chair Institutional Review Board
Date:	07/02/2007
Committee Action:	**Expedited Approval**
Approval Date:	07/02/2007
Review Type:	Expedited F7
IRB Protocol #:	0706001940
Study Title:	A Study of Unstructured Body Movements as a Basis for Design of Customized Products
Expiration Date:	06/27/2008

The above-referenced protocol was approved following expedited review by the Institutional Review Board.

It is the Principal Investigator's responsibility to obtain review and continued approval before the expiration date. You may not continue any research activity beyond the expiration date without approval by the Institutional Review Board.

Adverse Reactions: If any untoward incidents or severe reactions should develop as a result of this study, you are required to notify the Institutional Review Board immediately. If necessary a member of the IRB will be assigned to look into the matter. If the problem is serious, approval may be withdrawn pending IRB review.

Amendments: If you wish to change any aspect of this study, such as the procedures, the consent forms, or the investigators, please communicate your requested changes to the Institutional Review Board. The new procedure is not to be initiated until the IRB approval has been given.

Please retain a copy of this letter with your approved protocol.